FORMATION AND CHARACTERIZATION OF NANOFIBRILS FROM PEANUT PROTEIN

by

ALYSSA ROBERTSON

(Under the Direction of George Cavender)

ABSTRACT

Nanofibrils are protein aggregates formed under acidic and high temperature conditions that have a long fibrous appearance due to an internal structure of stacked beta-sheets. Proteins from milk, eggs, soybean, kidney bean, and pea, can form nanofibrils when held at proper conditions, but fibrils have yet to be formed from peanut proteins. The goal of this research was to determine if nanofibrils can be formed from peanut proteins and to characterize their formation kinetics, structure and functionality. Nanofibrils were formed under different conditions as determined using ThT fluorescence and TEM imaging. Nanofibrils are characterized as having shear thinning and viscosity enhancing behavior, and varying pH solubility. Such food protein nanofibrils could be important to the food industry as they might be used to stabilize or flocculate emulsions/foams, enhance viscosity, and form gel networks at lower protein concentrations than commonly used aggregates.

INDEX WORDS: Nanofibrils, Peanut protein, Electron microscopy, Rheology

FORMATION AND CHARACTERIZATION OF NANOFIBRILS FROM PEANUT PROTEIN

by

ALYSSA ROBERTSON

BS, University of Georgia, 2019

A Thesis Submitted to the Graduate Faculty of The University of Georgia in Partial Fulfillment of the Requirements for the Degree

MASTER OF SCIENCE

ATHENS, GEORGIA

2019

FORMATION AND CHARACTERIZATION OF NANOFIBRILS FROM PEANUT PROTEIN

by

ALYSSA ROBERTSON

Major Professor:	George Cavender
Committee:	Derek Dee
	Fanbin Kong

Electronic Version Approved:

Suzanna Barbour
Dean of the Graduate School
The University of Georgia
August 2019

ACKNOWLEDGEMENTS

I would like to thank my advisor, Dr. Dee, for mentoring and guiding me while learning to do research, work with new equipment, write my thesis, and communicate accurately with others. Without your help I would not have been able to accomplish this goal. I would, also, like to thank Dr. Cavender for stepping in and offering assistance once Dr. Dee moved schools. Your willingness to pick up where Dr. Dee left off in order to help me successfully finish the program was much appreciated. Thank you to all of my committee members for their knowledge, time, and helpful suggestions and comments.

I would like to thank my fellow lab mates: Ana, Lida, John, Clare, and Taryn, for helping me acquire equipment, training me on equipment, and showing me the inner workings of the laboratory.

I would like to thank Dr. John Shields at the University of Georgia Electron Microscopy center for offering advice, training, and equipment in order for me to acquire the TEM images necessary for the research.

Lastly, I would like to thank my parents, boyfriend, and friends for their constant support and advice. I honestly do not believe that I would have been able to accomplish this without everyone's help throughout graduate school.

TABLE OF CONTENTS

Page

LIST OF TABLES

Page

LIST OF FIGURES

Page

CHAPTER 1

INTRODUCTION

1.1 Protein Nanofibrils

Nanofibrils are characterized as fibrous, extracellular, proteinaceous deposits with an internal structure of beta-sheets stacked perpendicular to the fibril long axis (Nelson, et al, 2005). There are several diseases that are associated with nanofibril formation, such as Alzheimer's disease and type II diabetes which have raised concern for the use of fibrils in food products (Rambaran and Serpell, 2008). However, research on the cell toxicity of protein nanofibrils derived from kidney bean, soybean, whey, and egg white, illustrates that these fibrils have no detrimental effect on cell viability, suggesting that fibrils formed from food proteins could be used in food (Lasse et al, 2016). As mentioned, nanofibrils have previously been produced from whey, beta-lactoglobulin, oval albumin, hen egg white lysozyme, soybean, kidney bean, and pea proteins. Protein nanofibrils are formed by normally soluble proteins which amass into insoluble fibers (Perez et al, 2019). Fibril formation may occur upon partial denaturation and subsequent beta-sheet alignment, or, peptides from denaturation and hydrolysis assemble into the nanofibril structure (Chiti and Dobson, 2006). In the latter case, in order for partial denaturation and hydrolysis of the protein to occur, a protein solution is taken to a low pH (~2) and incubated at a high temperature (~65-85 °C).

1.2 Functionality in Food

The formation of nanofibrils shows promise for the food industry in that they have been found to enhance stabilizing or flocculate complex systems such as emulsions/foams, enhancing viscosity, and forming gel networks at lower protein concentrations than commonly used aggregates (Loveday et al, 2017; Kroes-Nijboer et al, 2012; Wan et al, 2016; Loveday et al, 2009). Fibrils have been shown to be beneficial in several food applications and advance food protein functionality (Cao and Mezzenga, 2019). The viscosity enhancing ability and shear thinning properties of soy fibrils have also been proposed as an agent that could be used to alter physical properties of food products (Akkermans et al, 2007). Pea protein fibrils and soybean fibrils have been illustrated to form gels that have comparable strength to each other but are weaker than gels formed with whey proteins (Munialo et al, 2014). As far as consuming and digesting food fibrils, fibrils from whey protein isolate (WPI), soybean protein isolate (SPI), and kidney bean protein isolate (KPI) have been found to be almost completely degraded by pepsin, pancreatin, and proteinase K. This digestibility of the food fibrils suggests that they should pose no harm to the human digestive tract and native protein structures. While some studies have looked at forming food fibrils from plants, the vast majority of research has focused on primarily dairy proteins and egg white. The desire to expand knowledge of fibril forming food proteins and to compare peanut protein fibrils to current studies on legume protein fibrils inspired this research.

1.3 Growing Interest in Plant Proteins

The food industry has increased its use of plant proteins as replacement for animal proteins, specifically milk, meat, and eggs, as these ingredients are relatively inexpensive and

consumers are looking to increase personal healthfulness, reduce environmental strain, and avoid allergens. As mentioned previously, a significant amount of research on food fibrils has dealt with animal proteins, but this research focuses on plant protein in order to gain a better understanding of fibrils formed from plants. In addition, there has been concern for using fibrils in food products because of the possibility of food fibrils inducing native human proteins into fibrils – possibly contributing to disease. The likelihood of this fibril induction is much smaller for plant protein fibrils than for animal-derived fibrils since human and animal proteins share more common characteristics than plant and human protein. Therefore, there is less chance for induction of native human proteins into fibrils with plant fibrils than with animal-derived fibrils (Araghi, 2018; Pimentel and Pimentel, 2003).

1.4 Plant Storage Proteins

Plant storage protein can be defined as proteins that are laid down at one stage in the plant's life cycle in order to be used in a future stage that is more metabolically active (Derbyshire et al, 1976). In legumes, the majority of storage proteins are characterized as salt-soluble globulins that can be further separated into legumins and vicilins. The individual names of the legumin and vicilin differ depending on the plant (Table 1), and legumin is typically the major storage protein of legumes, being differentiated from vicilin in several ways: it is not coagulated by heat, it contains disulfide bonds, it is non-glycosylated, and it undergoes post-translational cleavage into acidic and basic subunits. On the other hand, vicilin becomes coagulated at about 95 °C, contains no disulfide bonds, and is glycosylated (Derbyshire et al, 1976; Doyle et al, 1985). The two can be separated based on their sedimentation coefficients, 11S for legumin and 7S for vicilin.

Legumes are an essential part of global diets as they are considered the second most important source of foods for humans after cereals. They are significant because they are an inexpensive source of protein, starch, dietary fiber, vitamins, minerals, and polyphenols (Shevkani et al, 2015). Furthermore, some proteins and/or peptides of legumes are considered nutraceuticals in the food industry. Specifically, the 7S globulins of the common bean and soy and the 11S globulins of soy have been identified as nutraceuticals which have cholesterol/triglyceride lowering and hypotensive capabilities (Carbonaro et al, 2015).
The proteins of soybean, kidney bean, and pea have been found to form nanofibrils when held at proper conditions, such as low pH and high temperature, and these studies are reviewed below.

Table 1. Legume Protein Composition and Structural Characteristics

Source	Class	Common name	% of total protein	MW (kDa)	#Disulfide bonds	Glycosylation	Protein Data Base Files	References
Peanut	Legumin	Arachin	63	54.57	6	None	3C3V	Wang et al, 2014; UniProt, 2017; UniProt 2018
	Vicilin	Conarachin	33	48.09	0	Yes	3SMH	
Soybean	Legumin	Glycinin	60-75	55.71	8	None	1FXZ [1]	UniProt, 2017; UniProt 2018
	Vicilin	β-Conglycinin		50.44	0	Yes[2]	1UIJ [3]	
Kidney bean	Legumin	Legumin	Unknown	68.72	5	None	None	UniProt, 2017; UniProt, 2018
	Vicilin	Phaseolin	Unknown	47.57	0	Yes[4]	1PHS	
Pea	Legumin	Legumin	60	58.81	6	None	None	Munialo et al, 2014; Barac, et al, 2010; UniProt, 2017; UniProt, 2018
	Vicilin	Canavalin	Unknown	50.33	0	N53	2CAU	

1: proglycin subunit; 2: Located at N277, N551, N351; 3: beta subunit; 4: Located at: N252, N341

1.4.1 Soybean

In soybeans, the legumin is known as glycinin and the vicilin is known as β-conglycinin and together they compromise the globulin which makes up about 60-75% of the total protein (James and Yang, 2016). Glycinin is characterized as a hexamer of five subunits each with a basic and acidic subunit that is linked by a disulfide bond. The disulfide bonds are found at

positions 33 – 66 and 109 – 351 on the protein sequence (UniProt, 2017). β-conglycinin is a trimer composed of the alpha subunit, which is *N*-glycosylated at positions 277 and 551, an alpha prime subunit, and a beta subunit which is *N*-glycosylated at position 351 (UniProt, 2018; UniProt, 2017).

Of the several papers on legume protein nanofibrils, most have focused on soy protein and as a result, the techniques for formation are well-developed (Lasse et al, 2015; Akkermans et al, 2007; Wan and Guo, 2019; Dong et al, 2016; Wan et al, 2016; Xia et al, 2017; Josefsson et al, 2019; Purwanti et al, 2017; Warji et al, 2017). In general, nanofibrils can be formed from soybean by creating a solution of 10 mg/mL soy protein isolate in distilled water, using HCl to bring the pH to 1.6, and incubating the solution at 80 °C for 22 h (Lasse et al, 2015). The resulting fibrils have a curly structure, are about 8 nm wide, and 250-300 nm in length (Figure 1). Compared with whey protein fibrils, soybean fibrils are characteristically more branched and curlier than those from whey protein (Munialo et al, 2014). It is important to note that the images of the fibrils are heavily overlapping, suggesting that the width and length measurements might not be completely accurate.

It has also been discovered that β-conglycinin has a higher capacity to form fibrils than glycinin (Dong et al, 2016). Glycinin has disulfide bonds while β-conglycinin lacks any disulfide bonds, making the presence of disulfide bonds a possible inhibitor or limiter to the formation of fibrils. This could be a reason as to why β-conglycinin has a higher affinity for forming fibrils than glycinin (Dong et al, 2016). Furthermore, the subunits of β-conglycinin, alpha, alpha prime, and beta, all have different kinetics associated with fibril formation suggesting that the formation of nanofibrils is largely influenced by the amino acid sequence and structure of the protein itself (Dong et al, 2016).

As far as rheological behavior, fibrils formed from soy glycinin and SPI have been discovered to have shear thinning behavior and enhance viscosity compared to samples without fibrils with the SPI having higher viscosity than soy glycinin (Akkermans et al, 2007).

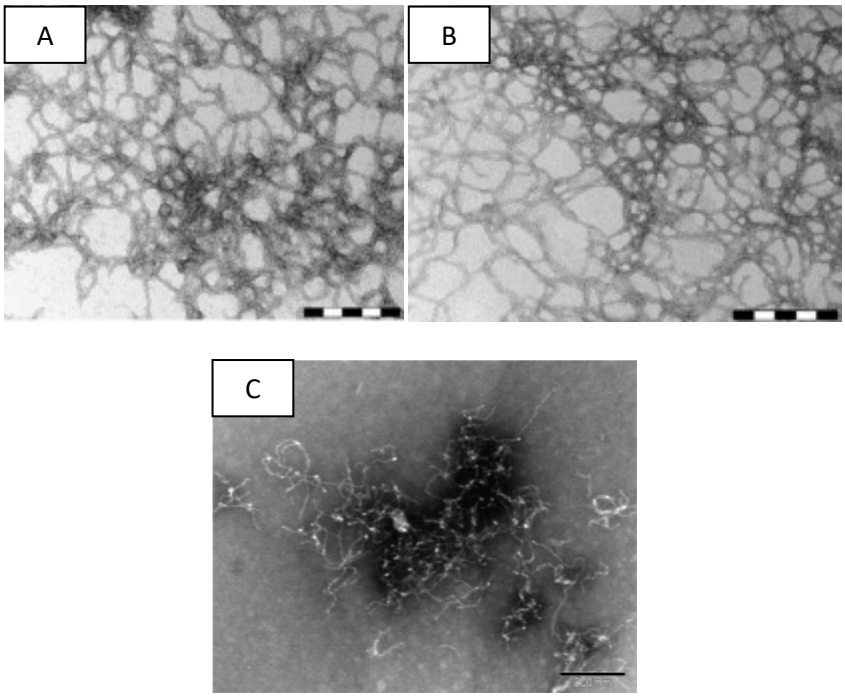

Figure 1. Transmission Electron Microscopy (TEM) Images of Nanofibrils Made from Different Legume Proteins. (A) soybean, (B) kidney bean, and (C) pea. [Panels A, and B were adapted from Lasse et al, 2016; Panel C was adapted from Munialo et al, 2014. All scale bars are 200 nm. Images reprinted with permission.]

1.4.2 Kidney Bean

Kidney beans contain about 20-30% protein and are lower in sulfur containing amino acids such as methionine and tryptophan compared to other legumes (Shevkani et al, 2015). In kidney beans, the legumin is not known by another name but the vicilin is called the phaseolin. Kidney bean legumin is characterized as a hexamer of five subunits each with a basic and acidic subunit that is linked by a disulfide bond (UniProt, 2017). Phaseolin makes up about 50% of the total protein and is composed of 3-5 subunits. Glycosylation occurs at positions N252 and N341 on the protein sequence (UniProt, 2018).

According to Lasse et al, 2016 and Tang et al, 2010, kidney bean fibrils can be formed the same way as soybean fibrils: by creating a solution of 10 mg/mL kidney bean isolate in distilled water, using HCl to bring the pH to 1.6, and incubating the solution at 80°C for 22 h. The resulting fibrils are also similar to soybean, being curly, about 8 nm wide, and 250-300 nm in length (Figure 1).

1.4.3 Pea

Peas contain roughly 20-25% protein and globulin makes up about 60% of that protein (Shevkani et al, 2015) (Gatel, 1994). In peas, the legumin is not known by another name but the vicilin is called the canavalin. Pea legumin is characterized as a hexamer of six subunit pairs, each with an acidic subunit of ~40 kDa and a basic subunit of ~20 kDa (Barac et al, 2010). Disulfide bonds occur at positions 31-64 and 107-339, the latter occurring between alpha and beta chains (UniProt, 2017; Munialo et al, 2014). Canavalin is a hexamer of three identical pairs of nonidentical subunits each defined by their molecular weights at ~30, ~34, ~47, and ~50 kDa and is glycosylated at position N53 (UniProt, 2018; Smith et al, 1982; Croy et al, 1980).

Fibrils can be formed from pea proteins by creating a solution of 40 mg/mL pea protein isolate and water, using HCl to bring the pH to 2.0, centrifuging at 15000 x g for 30 min in order to remove insoluble material, filtering the supernatant, using HCl to adjust the pH to 2.0 again, and incubating at 85°C for 20 h with continuous stirring at 300 rpm (Munialo et al, 2014). The resulting fibrils were characterized as being linear but twisted with a worm-like appearance and this was similar to the fibrils formed from soy β-conglycinin (Figure 1).

It has been determined that the formation of fibrils from pea protein follow the same general fibrilization mechanism as soy, specifically the hydrolysis of the protein into peptides

that assemble into the β-sheet alignment (Munialo et al, 2014). The exact region of the protein corresponding to the fibril core has not yet been determined and could be the next step in determining a proteins propensity to form fibrils. If a specific region can be isolated, then theoretically, any plant protein with that region/sequence should be able to form fibrils under similar conditions.

1.4.4 Peanut

Though considered a nut, peanuts are actually a legume and similar to all legume storage proteins (Table 1), in peanuts, globulin makes up the majority of the storage protein. It can be broken down into legumin and vicilin. In peanuts specifically, the legumin is called arachin and the vicilin is called conarachin. Arachin is a hexamer with each subunit having an acidic and a basic chain which are linked by disulfide bonds (UniProt, 2017). Arachin contains about 25% of the total amount of protein in peanuts, compared to conarachin which compromises about 8% of the total protein. (Johns and Jones, 1916). Conarachin contains about three times the amount of sulfur (1.09% as compared to 0.4% in arachin), contains more basic nitrogen (6.55% as compared to 4.96% in arachin), and is more soluble than the arachin, all of which aid in separating these two components (Johns and Jones, 1916).

A search of the literature yielded no reports on the formation of fibrils from peanut storage proteins, indicating that little research has been done in this area.

The individual protein sequence could have some effect on the formation of fibrils and could explain slight differences in the methods of fibril formation and/or the characterization of the resulting fibrils. While vicilin has been shown to form nanofibrils at a higher rate than

legumin in soybean, possibly due to the presence of disulfide bonds, fibrils can still be formed from the protein without separating the two fractions (Josefsson et al, 2019).

1.5 Objective

Although soybean, kidney bean, and pea proteins are known to form fibrils, to our knowledge there have been no reports describing nanofibrils formed from peanut proteins. Given that peanuts contain a high proportion of legumin and vicilin proteins, and that these proteins share a conserved folded structure with other legumes, it is likely that peanut proteins can also form nanofibrils. The objective of this research was four-fold: 1) To determine if nanofibrils could be formed from peanut proteins under similar conditions to other legume fibrils, 2) To gain fundamental knowledge about how storage proteins form fibrils, 3) To compare peanut protein fibril formation and characteristics to known legume protein fibrils, and 4) To measure rheological properties of peanut protein fibrils in order to predict potential functionality for the food industry.

CHAPTER 2
MATERIALS AND METHODS

2.1 Materials

Raw peanuts of the Runner variety from Hampton Farms, Inc. (Severen, NC, USA) were purchased from a local grocery store (Bell's Food Store, Athens, GA, USA). Thioflavin T (ThT) (CAS #: 2390-54-7) was purchased from Sigma-Aldrich (St. Louis, MO, USA). All other reagents, including Tris(hydroxymethyl)aminomethane (Tris), Tricine, Hydrochloric acid, Sodium hydroxide, Bovine-Serum Albumin (BSA), Coomassie G-250/R-250 stain, Uranyl acetate, Laemmli sample buffer, Tricine sample buffer, Tris-Tricine running buffer, Tris-Glycine running buffer, and Dithiothreitol (DTT) were of ACS Reagent grade or higher, and were purchased from Thermo Fisher Scientific (Waltham, MA, USA).

2.2 Protein Extraction

Proteins were extracted from the raw peanuts, using a method adapted from Koppelman, et al (2001) in order to isolate the protein to form fibrils. Briefly, de-shelled, de-husked peanuts were ground using a food processor to create a powder and 3 g of the resulting ground peanut powder was mixed for 2 hours at room temperature (RT) with 30 mL of 20 mM Tris(hydroxymethyl)aminomethane Hydrochloride (Tris-HCl) buffer at pH 8.2. The resulting solution was centrifuged at 3000 x g for 10 minutes in an ultra centrifuge (Sorvall^{TM} RC6 Plus, ,Thermo Scientific (Waltham, MA, USA) to remove any insoluble particles and after decanting, the supernatant was centrifuged at 12000 x g for 20 minutes to remove fat. This extract was then either stored at 4 ℃ for later use or used immediately as described below.

2.3 Protein Concentration

Protein concentration was estimated in order to gain an understanding of the protein concentration of the peanut protein extract used in the formation of fibrils. A protein concentration was measured using a Bradford Assay according to the method described by Bio-Rad Laboratories (n.d.). Briefly, five protein samples were made by extracting the peanut protein according to the method above, then, seven standards (concentrations 20 mg/mL, 17.5 mg/mL, 15 mg/mL, 12.5 mg/mL, 10 mg/mL, 5 mg/mL, and 2.5 mg/mL) were created using Bovine Serum Albumin (BSA) diluted with 20 mM Tris-HCl buffer at pH 8. Each standard was mixed with 1x Coomassie G-250/R-250 stain and a blank sample was created using water and 1x Coomassie G-250/R-250 stain. All samples were incubated at room temperature for at least 5 min. Using a UV-Vis Spectrophotometer (Nanodrop™ One Microvolume ,Thermo Fisher Scientific, Waltham, MA, USA) set to the manufacturer provided Bradford Assay setting, the instrument was zeroed using the blank sample. Then, the absorbance of each BSA standard was measured at 595 nm in triplicate. Next, samples of peanut protein extract with unknown concentration were mixed with 1x Coomassie G-250/R-250 stain and loaded several times onto the lower measuring pedestal where 4-5 absorbance measurements per sample were collected. The spectrometer pedestal was cleaned with DI-H_2O between each sample. A standard curve was created by plotting the absorbance at 595 nm values of the BSA standards versus the concentrations of the BSA standards. The unknown concentrations of the peanut protein samples were determined using the curve based on their absorbance at 595 nm.

Protein concentration was also determined based on absorbance at 280 nm using the same spectrophotometer. Using the A280 function on the instrument, the estimated extinction coefficient was entered, and Beer's Law was used to calculate approximate protein concentration

based on amount of absorbance at 280 nm. The extinction coefficient of the peanut protein was estimated to be 32,851 M^{-1} cm^{-1}, calculated by using a weighted average of the published extinction coefficients and relative concentrations of the two major peanut proteins, arachin, 44,850 M^{-1} cm^{-1} (UniProtKB – Q647H2; Gasteiger et al, 2005) and conarachin, 9,970 $M^{-1}cm^{-1}$ (UniProtKB – Q6PSU4; Gasteiger et al, 2005) at 65.6% and 34.4%, respectively (Wang et al, 2014). The samples measured were made by the protein extraction method mentioned previously and by doubling the starting raw peanut powder and halving the starting raw peanut powder in order to create fibril solutions that varied in protein concentration by factors of 0.5, 1, and 2.

2.4 Fibril Formation Conditions

Peanut extract was brought to pH 2.0 using HCl and then centrifuged at 15000 x g for 30 minutes in order to remove any insoluble particles that resulted from the pH change. Then, 2 mL of protein extract was put into 1-dram (3.7 mL) vials and held at either 65 °C or 80 °C in a hotplate/ stirrer with stirring at 400 rpm (Profession Round Top , VWR® Radnor, PA, USA). A total of eight trials were performed in order to observe the rate of fibril formation under different conditions. For two trials, 8 vials were heated at 65 ℃ with 4 vials stirring and 4 vials without stirring. For another two trials, 8 vials were heated at 80 ℃ with 4 vials stirring using stir bars and 4 vials without stirring.

Four more trials were completed at 65 ℃ and 80 ℃, each, with all 8 vials stirring using stir bars for the first 10 hrs, then 4 of the vials continued to stir and the other 4 vials were set at room temperature for 7 days. These trials were done in order to determine if the condition under which fibrils were formed could be manipulated in order to maximize fibril length. During the incubation period, aliquots of 400 μL were taken at time zero and every 2.5 hrs for the first 24

hrs and then every 24 hrs afterwards for one week, with all aliquots being stored at 4 ℃ until further analysis.

2.5 Thioflavin T (ThT) Fluorescence

ThT fluorescence was utilized in order to observe the formation of nanofibrils from the peanut protein solution. Nanofibrils were detected based on their interaction with the dye Thioflavin T (ThT) and the resulting increase in ThT fluorescence (Xue et al, 2017). ThT binds with beta-sheet rich structures, such as nanofibrils, and once bound, the fluorescence emission wavelength of ThT shifts from ~510 nm to ~480 nm. If fluorescence emission occurs at this wavelength, then nanofibrils have most likely formed as ThT will not emit a signal at 485 nm unless bound to beta-sheet rich structure (Malmos et al, 2017). The aliquots of the incubated protein extracts were placed in a fluorescence cuvette along with 20 mM Tris-HCl buffer at pH 2.0 and 20 mM ThT. The fluorescence of the solution was recorded using a fluorescence spectrophotometer (Cary Eclipse, Agilent Technologies,Santa Clara, CA USA) using an excitation wavelength of 460 nm and measuring an emission spectrum from 450 nm – 550 nm. A graph of the intensity over time was created in order to depict the kinetics of fibril formation and the kinetics can be compared for fibrils formed under different conditions. The rate of formation was also determined and compared at different conditions. The ThT fluorescence time progress curves were fit according to equation 1, after the methodology of Arosio, Knowles, & Linse, (2015) using IGOR Pro data analysis software (WaveMetrics, IncPortland, OR, USA).

$$y = y_0 + A/(1 + e^{-k(t-t_{0.5})}) \qquad \text{eq [1]}$$

y_0 is the y-intercept, k is the rate constant, and $t_{0.5}$ is the half-time, and is related to the lag phase, t_{lag}, using equation 2.

$$t_{lag} = t_{0.5} - 1/2k \qquad \text{eq [2]}$$

2.6 TEM Imaging

Electron Micrographs of the fibrils formed under different conditions were taken using a Transmission Electron Microscope (JOEL JEM 1011, JEOL, Inc., Peabody, MA, USA) in order to compare characteristics of the fibrils, such as length, width, and persistence length. The extract containing fibrils was plated on TEM grids at time periods initially after and several days after initial fibril formation in order to observe the fibrils over time. Plating was done by loading 5 µL of the desired sample onto a TEM grid, allowing sample to sit for 5 minutes, then being wicking off excess liquid using Whatman No. 4 filter paper. Each grid was then washed twice with deionized water, again wicking off using filter paper after each wash. Samples were then negative stained by dispensing 5 µL of uranyl acetate on the grid and waiting 30 seconds before wicking it off with filter paper. The morphology for the fibrils formed under different conditions were compared since fibrils have been known to be short, long, curly, straight, wide, narrow, etc. For each condition, between 10 – 20 images were collected. Using ImageJ Software (U. S. National Institutes of Health, Bethesda, Maryland, USA,), the average length and width of fibrils formed was identified and compared. Persistence length, the measure of a polymer's resistance to bending, was also determined, as it gives a good idea of the polymer's structural rigidity and the amount of energy needed to deform it (Manning, 2006). This was accomplished using the methodology and software developed by Graham, et al (2014) and the method was repeated for

each of the different conditions in order to determine meaningful comparisons. Length and widths were analyzed for statistical significance via multi-way analysis of variance and Fishers LSD post hoc testing as appropriate using statistical software (SAS v15.1, The SAS Institute, Cary, NC). Results were considered to be different if $\alpha<0.05$.

2.7 SDS-PAGE

SDS-PAGE gels were prepared in order to compare the extent of acid hydrolysis on the proteins over time. Both Precast Protein Gels (4 – 20% Mini-PROTEAN® TGX™ Bio - Rad Hercules, CA, USA and Tris/Tricine Precast Gels (Mini-PROTEAN®, Bio - Rad Hercules, CA, USA) were used to qualitatively determine different molecular weight fractions.

The 4 – 20% Mini-PROTEAN® TGX™ Precast Protein Gels were loaded with samples that had been incubated at 80 ℃ and 65℃ while stirring, with aliquots taken at time zero, 1 hr, 2.5 hr, 5 hr, 10 hr, 24 hr, 72 hr for 80 ℃, 96 hr for 65 ℃, and 168 hr. For each time point, 3 µL of sample were diluted with 47 µL deionized water and vortexed to mix thoroughly. After mixing, 10 µL of the sample and deionized water mixture were diluted with 20 µL Laemmli sample buffer containing DTT to get an approximate final protein concentration of 0.1 µg/µL.

Mini-PROTEAN® Tris/Tricine Precast Gels were loaded with samples incubated at 80 ℃ and 65 ℃ while stirring, with aliquots taken at the previously described times. For each time point, 3 µL of sample were diluted with 47 µL deionized water and vortexed to mix thoroughly. After mixing, 10 µL of the sample and deionized water mixture were diluted with 20 µL Tricine sample buffer containing DTT to get an approximate final protein concentration of 0.1 µg/µL.

Additionally, in order to separate and identify the peptides that compromised the fibril , gels were also loaded with spin-filtered samples, comprising 5 µL aliquots of samples which

were incubated at 80 ℃ with stirring from time zero and 24 hr, which were then diluted with 45 µL of deionized water and vortexed. Then, 10 µL of the water and sample mixture was diluted with 40 µL of Tris-Tricine sample buffer. Half of each 24 hr sample was loaded into 100 kDa spin filters placed in 0.5 mL microcentrifuge tubes and centrifuged at 10 x g for 4 min, then one was rinsed with pH 2 buffer and the other was rinsed with pH 8 buffer. The supernatant of each were collected by flipping the spin filter upside into a clean microcentrifuge tube and centrifuging at 1.0 x g for 2 minutes. This procedure was designed to allow the spin filters to remove any protein or substance that was in the protein fibril solution but did not participate in fibril formation. The different pH buffer rinses of the filters were used in order remove any intact trimer/hexamer that could have been retained alongside the walls of the filter.

All samples were heated at 95 ℃ for 5 minutes using an incubator then 5 µL of each sample and 8 µL of ladder were loaded onto the desired gel. The 4 – 20% Mini-PROTEAN® TGX™ Precast Protein Gels ran for 20 minutes at constant 200 V with Tris-Glycine running buffer and the Mini-PROTEAN® Tris/Tricine Precast Gels ran for 90 minutes at 125 V with Tris-Tricine running buffer. Afterwards, gels were placed on an oscillating table and fixed with a 40% methanol/10% acetic acid solution for 3 hours. Then, the fixing solution was removed, and the gels were stained with 0.25 % Coomassie G-250/R-250 stain for 1 hour. Finally, the stain was removed, and the gels were destained in deionized water overnight and images were taken of the gels.

2.8 Functional Studies

2.8.1 pH solubility

The purpose of this was to determine at which pH the fibril was least soluble. Fibrils were created as described previously and incubated for 20 hrs at 65 ℃. After the incubation period, the samples were transferred into 15 mL centrifuge tubes and adjusted to pH 4, 6 and 8 using NaOH. The samples were then stirred at room temperature using stir bars for 30 minutes, then centrifuged at 10,000 rpm for 30 minutes. The supernatant and pellet were collected for each pH and ThT fluorescence data was collected for all supernatants by the same method mentioned previously and for all resolubilized pellets. Pellets were resolubilized in 20 mM Tris-HCl buffer at pH 2, 4, 6, or 8, depending on the pH of the sample, at a volume twice as much as the pellet. Absorbance at 280 nm was also measured for all supernatants and pellets and was used to determine the relative concentration of protein in each sample. The % total signal was found for each supernatant and pellet at each pH by calculating the proportion of ThT signal for either the supernatant or pellet compared to the total signal (supernatant + pellet) in order to determine where fibrils were present. UV 280 nm was found by using the Nanodrop1 following the same method as the A280 nm method in order to determine concentration of protein in each supernatant and pellet at different pHs. The % of Total Protein was found for each supernatant and pellet at each pH by calculating the proportion of protein concentration according to absorbance at 280 nm for either the supernatant or pellet compared to the total protein concentration (supernatant + pellet) in order to determine what percentage of protein made up the supernatant and pellet at each pH.

2.8.2 Rheology

Fibrils were created using the general methods described previously but with relative protein concentrations of 0.5-fold, 1-fold, and 2-fold, which were made by either halving or doubling the starting raw peanut powder. After incubation at both 65 ℃ and 80 ℃ stirring for 24 hrs the samples were collected and the shear rate, shear stress, and viscosity were measured on each sample using a Hybrid stress/strain-controlled Rheometer (Discovery HR-2 TA Instruments New Castle, DE, USA) with cone/ plate geometry and rate sweeps with shear rates varying between 0.01 and 100 s^{-1}. The data collected by the manufacturer's software were used to generate graphs of shear rate vs shear stress and shear rate vs viscosity, allowing the determination of the potential viscosity enhancing and shear stress properties of fibrils formed under different conditions in order to further explain the functionality of the fibril.

CHAPTER 3

RESULTS

3.1 Protein Concentration

As shown in Table 2, for the protein concentration determined using the Bradford Assay, the average concentration for the protein extracted from the raw peanut was approximately 5.64 mg/mL. For the protein concentration determined using absorbance at 280 nm on the Nanodrop, the approximate protein concentration for the 1/2x sample was 13.96 mg/mL, for the 1x sample was 24.46 mg/mL, and for the 2x sample was 36.49 mg/mL. The reason for the samples not being exactly ½ and 2x the middle sample could have arisen in improper sampling, weighing, loss of material during transfers, and not completely extracting all of the protein from the raw peanut. The 1x sample was made exactly the same as the samples measured using the Bradford Assay. The protein concentration of the fibril samples used in this experiment are in the range of 5 mg/mL and 40 mg/mL unless stated otherwise.

The difference in results from the Bradford assays and absorbance at 280 nm are most likely due to the fact that the protein extraction method did not result in a purified protein. While arachin and conarachin make up the majority of the peanut protein, there are other minor proteins that could have resulted in interference. Further, the estimated extinction coefficient utilized was based on the idea that the extraction was made up of 65.6 % of arachin and 34. 4% conarachin which may be inaccurate because the exact composition of the extraction was not determined.

Table 2. Table 2: Protein Concentration Estimate Using Bradford Assay and A280 methods

Assay Method[1]	Protein Content(mg/mL)[2]	Absorbance[3]
Bradford (1 X)	5.64 ±.16.35	1.37 ± 0.11
A280 (½ X)	13.96 ± 0.17	9.35 ± 0.12
A280 (1 X)	24.46 ± 5.91	16.39 ± 3.96
A280 (2 X)	36.49 ± 5.97	24.45 ± 4.00

1: 1X=extract prepared from 3 g powdered peanut per 30 mL buffer, ½ X = extract prepared from 1.5 g powdered peanut per 30 mL buffer, 2 X = extract prepared from 3 g powdered peanut per 30 mL buffer
2: Mean values, ± standard deviation, n = 3
3: Mean values, as measured at a wavelength of 595 nm (Bradford) or 280 nm (A280), according to describe method, n = 3

3.2 ThT Kinetics

ThT kinetics for each condition were determined by fitting the ThT fluorescence intensity vs time results for each condition to equation 1. This was done in order to demonstrate the rate of which fibrils were forming and the time length of the lag phase before formation at each condition.

As seen in Figure 2, graphs B and C, for both temperatures, 65 ℃ and 80 ℃, under the condition of constant stirring, the curves had sigmoidal shape. Also, ThT fluorescence intensity increased by about 8-fold from time zero for 65 ℃ and about 6-fold from time zero for 80 ℃ suggesting that fibrils were formed. For both temperatures, it appeared that formation was completed between 10 and 24 hrs, as illustrated by a constant ThT intensity. For both 65 ℃ and 80 ℃, ThT fluorescence intensity for samples without stirring did not increase suggesting that fibril formation did not occur.

The average rate constant was highest for samples incubated at 80 ℃: 0.89 ± 0.40 h^{-1} followed by samples incubated at 65 ℃: 0.54 ± 0.30 demonstrating that the rate of formation was highest at 80 ℃ compared to 65 ℃ which is supported by the ThT fluorescence data. The lag phase was lowest for samples incubated at 80 ℃: 3.64 ± 1.10 followed by samples incubated

at 65 ℃: 5.81 ± 3.80 demonstrating that the lag phase is shortest for fibrils incubated at higher temperatures.

For the trial where half the samples were kept at room temperature and half were kept at 65 ℃, the ThT fluorescence intensity kinetics were comparable over the first 10 hrs, showing not much difference in intensity or time of formation between conditions, while the sample that continued stirring and heating showed increasing fluorescence out to 160 hrs (Figure 4 and Figure 5).

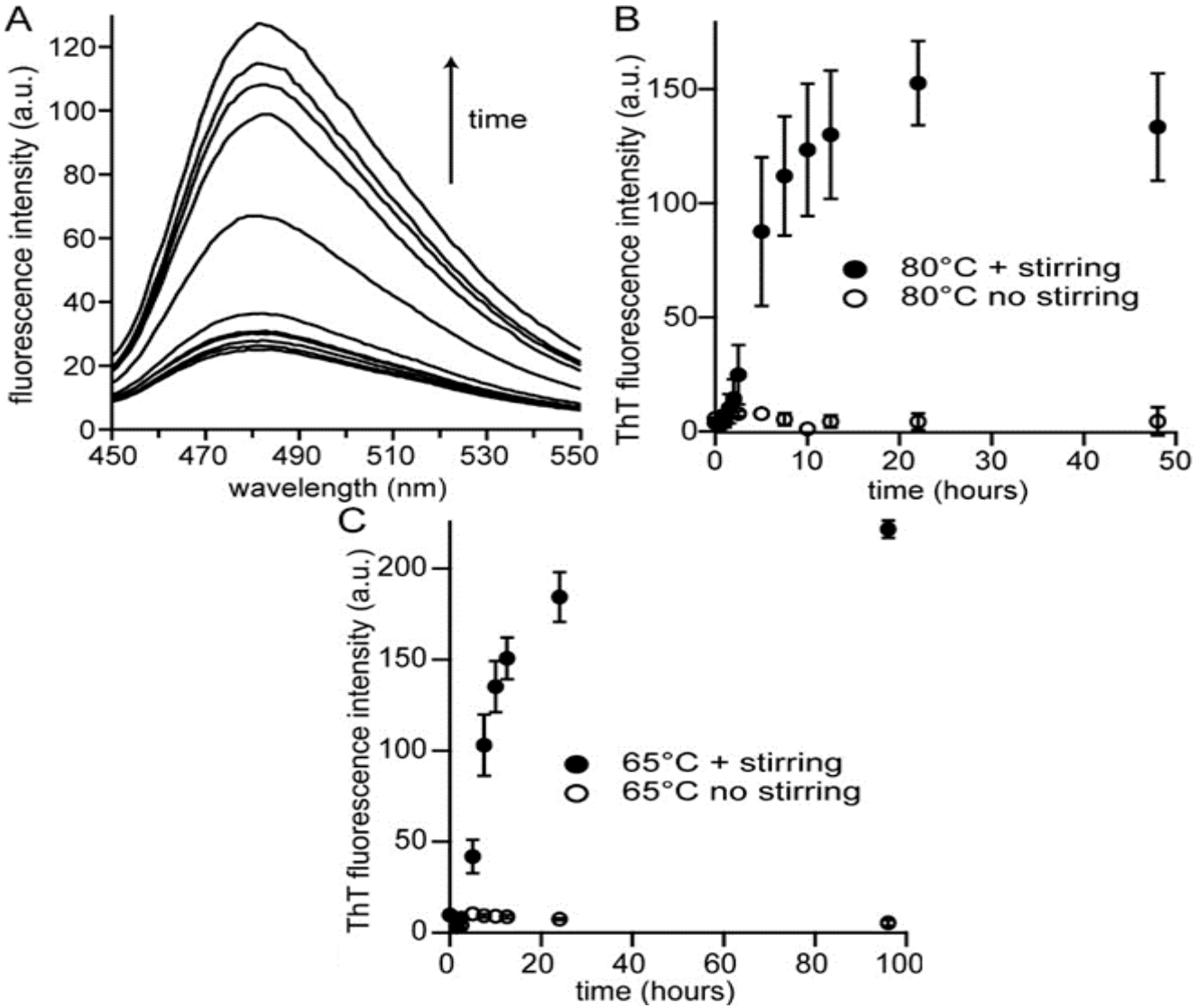

Figure 2. Peanut Protein Nanofibril Growth Measured Using ThT Fluorescence. (A) ThT fluorescent emission intensity increased over time. 20 uM ThT was combined with peanut protein extract (30 mg/ml) that was incubated at 80 °C, pH 2.0, with stirring. (B and C) The increase in ThT fluorescence over time, with and without stirring, at (B) 80 °C and (C) 65 °C.

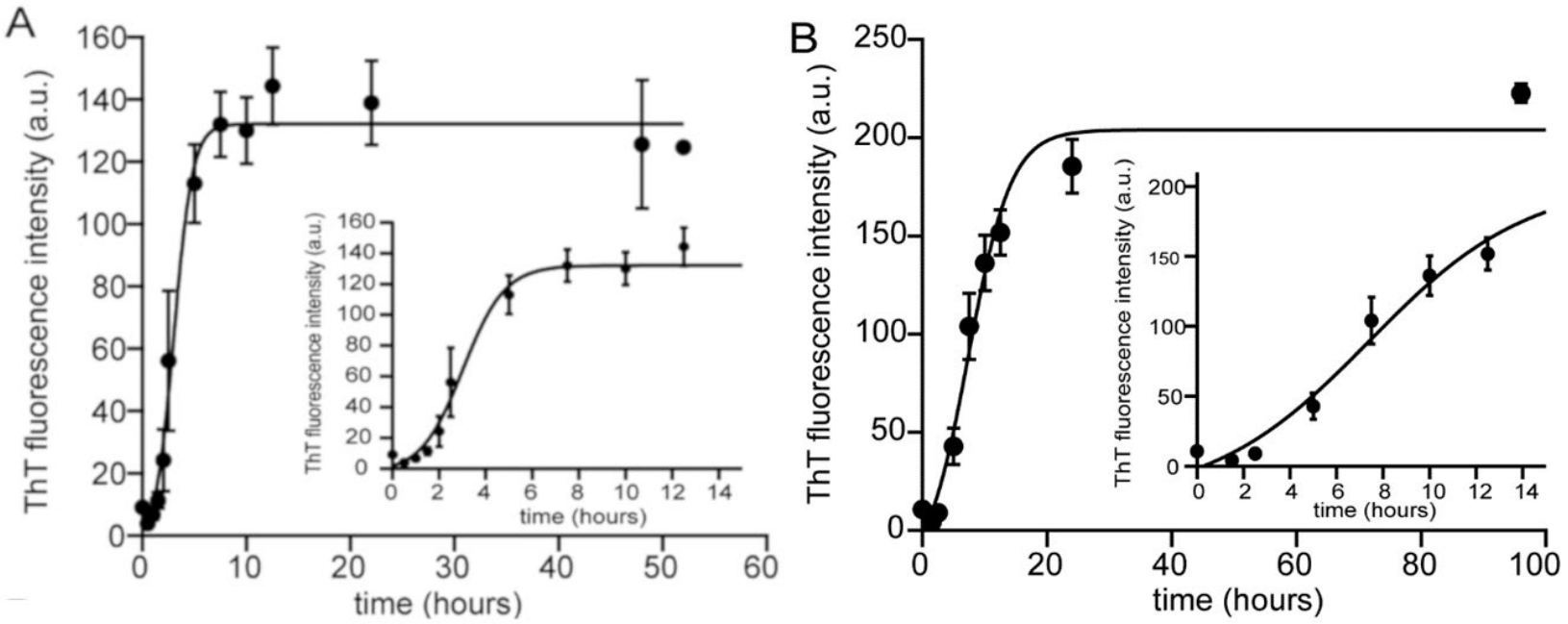

Figure 3. Kinetics of Peanut Protein Nanofibril Formation. At 80 °C (A) and 65 °C (B), pH 2.0, with stirring. Insets show a close-up of the first 15 h of each reaction. The lines correspond to fits of the data using equation 1.

Table 3. Fitting Results from ThT Fluorescence Kinetics (equation 1).

	k (h^{-1})	**t_{lag} (h)**
80 °C average*	0.89 ± 0.40	3.64 ± 1.10
65 °C average*	0.54 ± 0.30	5.81 ± 3.80
* n= 8		

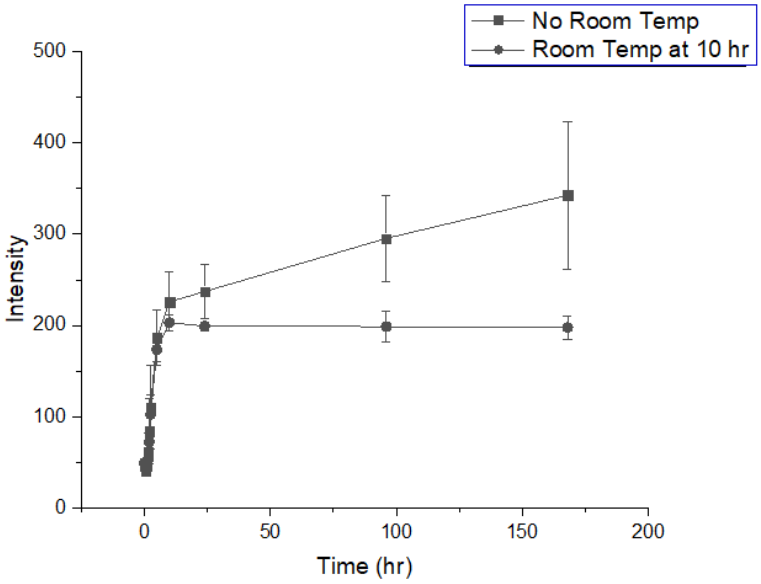

Figure 4. ThT kinetics for Room Temperature Trial. Samples heating at 65 ℃ stirring for 10 hrs, then half moved to room temperature and the other half continued to stir at 65 ℃.

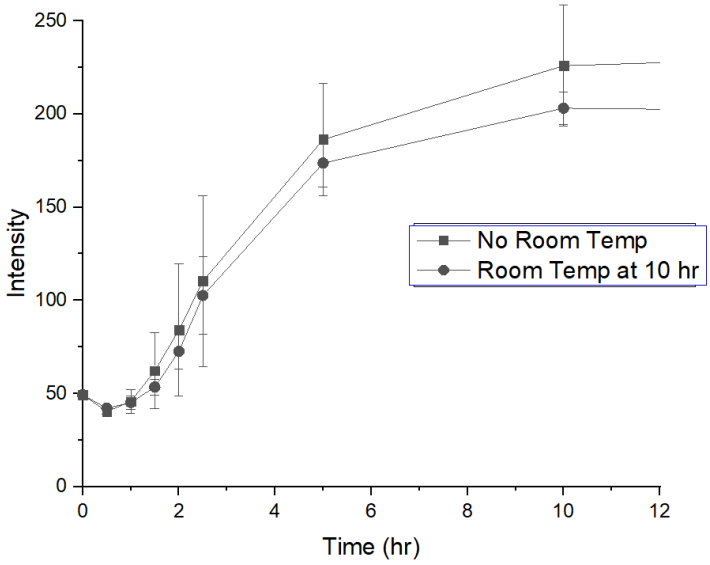

Figure 5. Close-Up of Lag Phase of Figure 4 - ThT kinetics for samples heating at 65 ℃ stirring for 10 hrs, then half moved to room temperature and the other half continued to stir at 65 ℃.

3.3 TEM Imaging

Transmission Electron Microscopy images, shown in Figures 6 - 12 confirm the formation of peanut protein nanofibrils. Table 4 highlights the mean measurements of the observed fibrils, including length, width and persistence length. Briefly, for both temperatures, over time, conditions without stirring appeared to result in longer and wider fibrils on average. For both temperatures, over time, conditions with stirring appeared to result in shorter but wider fibrils on average. Further, fibrils formed at 65 ℃ were on average, both longer and wider than fibrils formed at 80 ℃, most likely due to a more complete breakdown of the fibrils in the more extreme environment.

Further, fibrils initially incubated at 65 ℃ with stirring for 10 hrs and then room temperature storage for the remaining 24 hrs, appeared, on average, longer, wider, and had a higher persistence length than fibrils incubated at 65 ℃ stirring for the entire 24 hrs. Fibrils initially incubated at 65 ℃ with stirring for 10 hrs and then room temperature storage for the remaining 24 hrs, appeared, on average, longer than fibrils incubated at 65 ℃ stirring for the entire 24 hrs but had similar widths and persistence lengths. For fibrils incubated at 65 ℃ not stirring, the average persistence length increased with time. For fibrils incubated at 65 ℃ stirring, the average persistence length increased after 10 hrs then slightly decreased after 24 hrs. For fibrils incubated at 80 ℃ not stirring, the average persistence length decreased over time. For fibrils incubated at 80 ℃ stirring, the average persistence length increased over time.

Fibrils formed at 65 ℃ not stirring after 2.5 hrs were significantly different in length than fibrils formed at 65 ℃ not stirring after 24 hrs, showing that fibrils became longer over time without stirring; they were also significantly different than 80 ℃ not stirring after 2.5 hrs, showing that fibrils were longer at lower temperatures initially. Fibrils formed at 65 ℃ not

stirring after 24 hrs were significantly different in length than fibrils formed at 65 ℃ stirring after 24 hrs, showing that fibrils formed without stirring are longer than those formed with stirring. Fibrils formed at 80 ℃ not stirring after 2.5 hrs were significantly different in length than fibrils formed at 80 ℃ stirring after 2.5 hrs showing that fibrils are longer initially when under stirring conditions. Fibrils formed at 80 ℃ not stirring after 24 hrs were significantly different in length than fibrils formed at 80 ℃ stirring after 24 hrs showing that fibrils, once again, became longer over time. Fibrils formed at 80 ℃ stirring after 24 hrs were significantly different in length than fibrils formed at 80 ℃ room temp after 24 hrs showing that bringing the fibrils to room temperature after initial incubation results in longer fibrils. There were no statistically significance differences in fibril width under any condition.

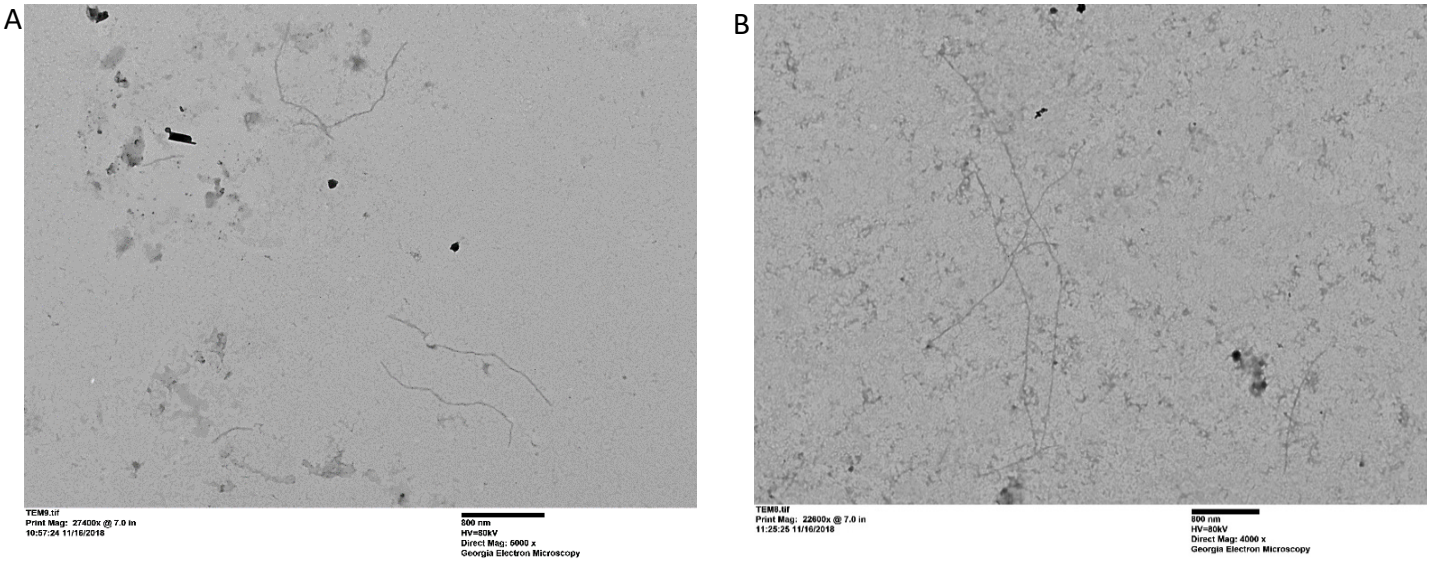

Figure 6. Structure of Peanut Protein Amorphous Aggregates and Nanofibrils Formed at 65 °C, no stirring Observed using TEM: after (A) 2.5 hr and (B) 24 hr.

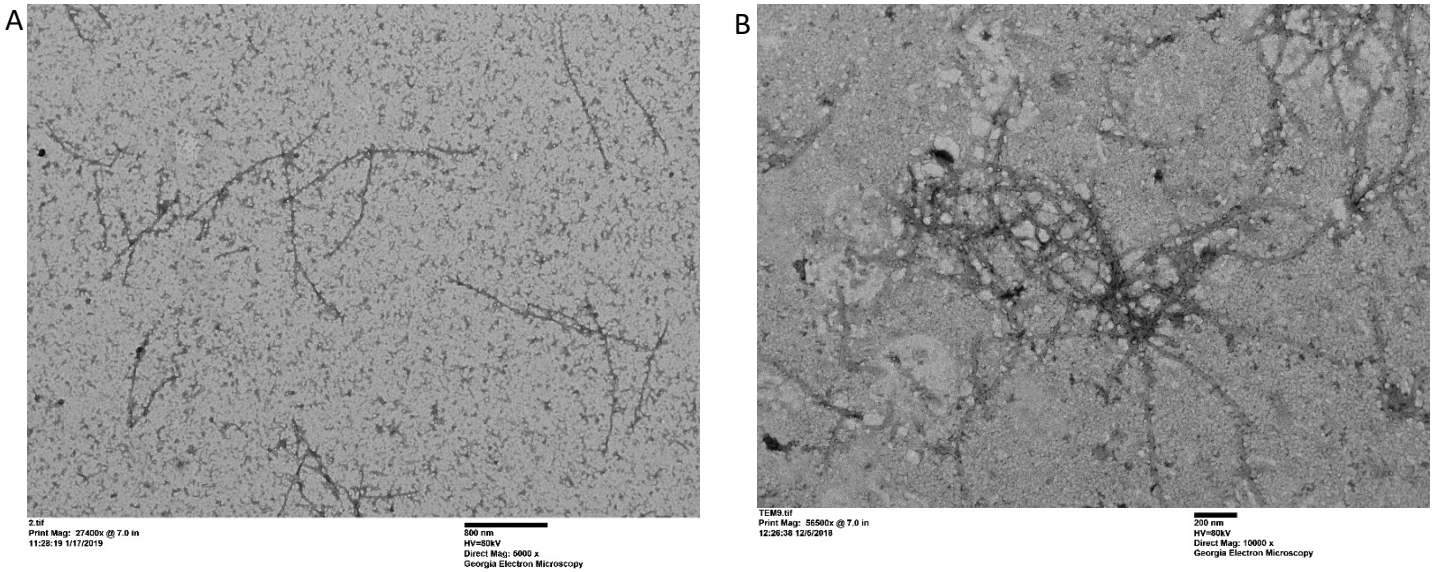

Figure 7. Structure of Peanut Protein Amorphous Aggregates and Nanofibrils Formed at 65 °C, stirring Observed using TEM: after (A) 2.5 hr and (B) 24 hr, with stirring.

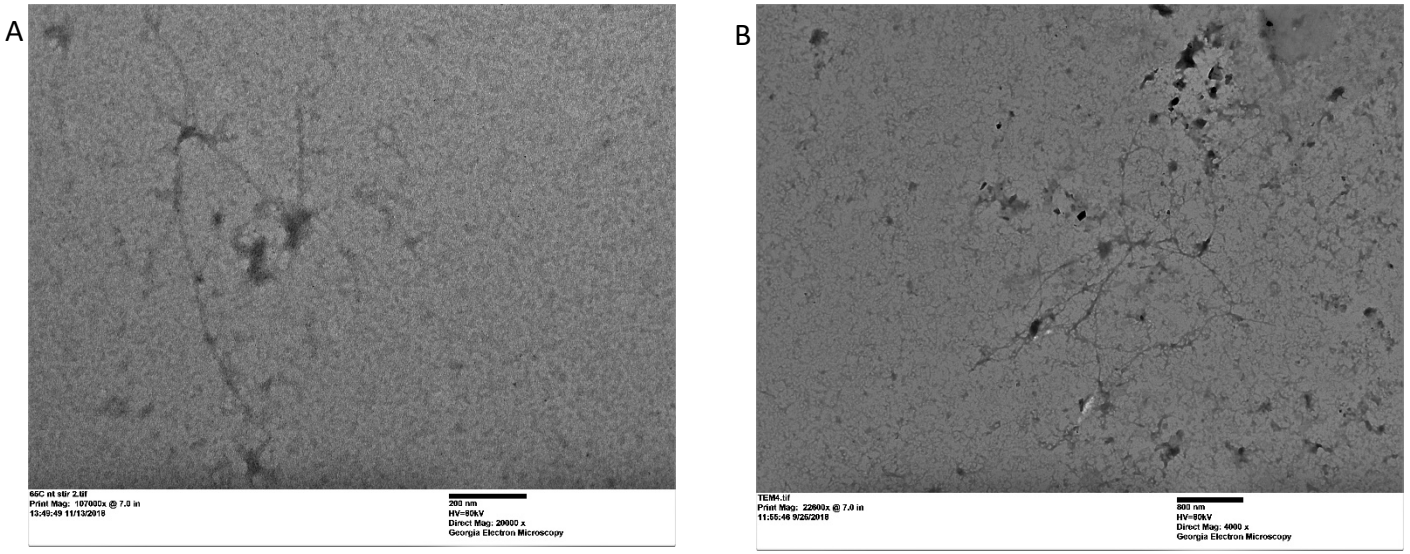

Figure 8. Structure of Peanut Protein Amorphous Aggregates and Nanofibrils Formed at 80 °C, no stirring Observed using TEM: after (A) 2.5 hr and (B) 24 hr.

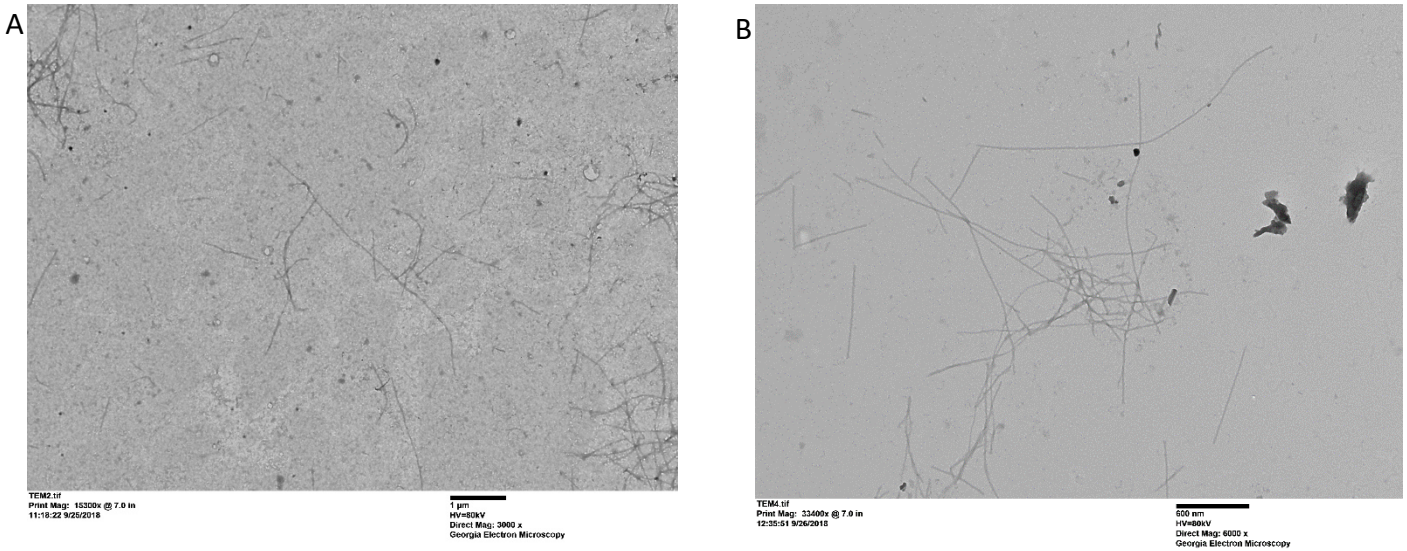

Figure 9. Structure of Peanut Protein Amorphous Aggregates and Nanofibrils Formed at 80 °C, stirring Observed using TEM: after (A) 2.5 hr and (B) 24 hr.

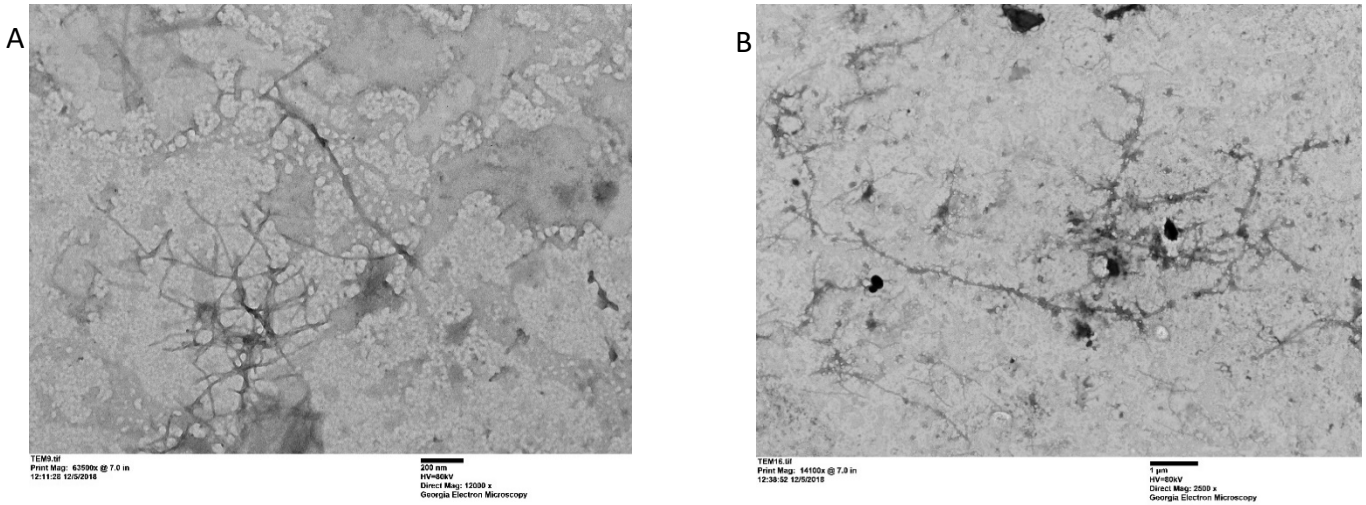

Figure 10. Structure of Peanut Protein Amorphous Aggregates and Nanofibrils Formed at 65 °C, stirring Observed using TEM: after 24 hrs at room temperature (A) and after 65 °C stirring for 10 hrs, then room temperature for 24 hrs (B).

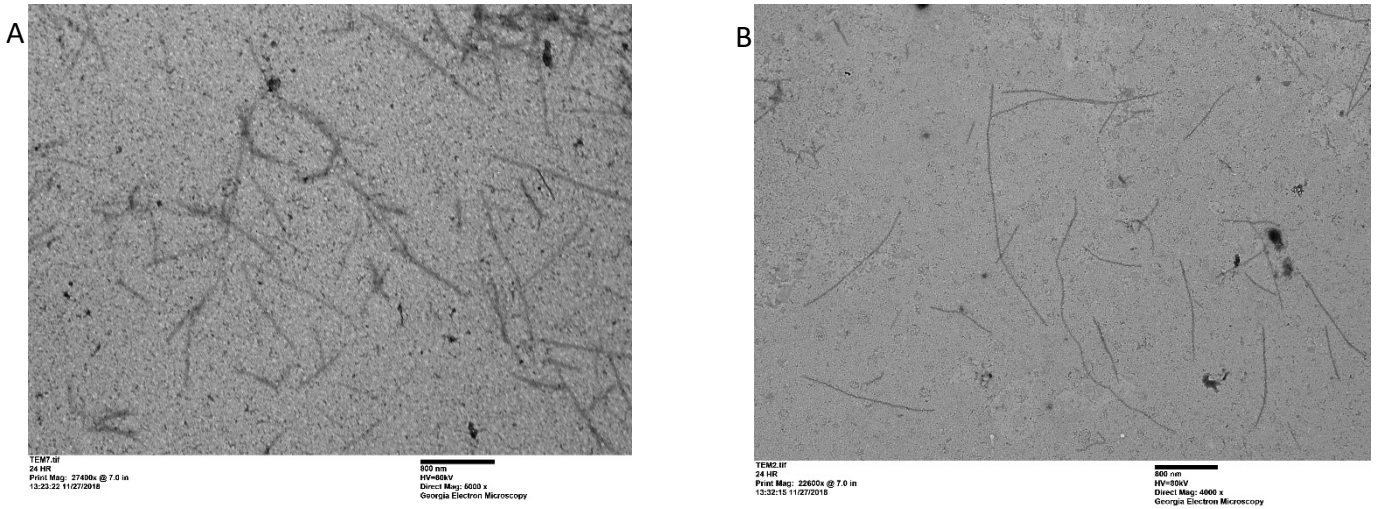

Figure 11. Structure of Peanut Protein Amorphous Aggregates and Nanofibrils Formed at 80 °C, stirring Observed using TEM: after 24 hrs at room temperature (A) and after 80 °C stirring for 10 hrs, then room temperature for 24 hrs (B).

Table 4. Structural Parameters Obtained from Analysis of TEM Images.

Condition	Time (h)	n	Length (nm)	Width (nm)	Lp (µm)
65 ℃ not stirring	2.5	12	1669.51 ± 904.20^{C}	23.10 ± 5.23^{AB}	2011.92
	24	8	3488.16 ± 2076.36^{A}	24.59 ± 5.68^{AB}	3747.23
65 ℃ stirring	2.5	21	1540.95 ± 642.06^{CD}	19.71 ± 4.82^{AB}	2247.64
	10	13	1166.22 ± 525.24^{CD}	22.11 ± 2.75^{AB}	3154.73
	24	19	799.61 ± 523.41^{D}	30.80 ± 30.65^{A}	2521.89
80 ℃ not stirring	2.5	5	664.05 ± 376.10^{D}	11.80 ± 3.18^{B}	2778.77
	24	5	2794.90 ± 727.36^{AB}	19.69 ± 6.06^{AB}	2402.02
80 ℃ stirring	1	7	1497.06 ± 597.84^{DC}	27.64 ± 6.62^{A}	1650.47
	2.5	10	1803.80 ± 1521.99^{BC}	30.31 ± 9.84^{A}	2556.30
	24	37	957.01 ± 376.76^{D}	21.11 ± 5.69^{AB}	3134.70
65 ℃ 10 hrs, RT 24 hrs	24	28	1449.88 ± 1442.88^{DC}	27.67 ± 11.66^{A}	2605.95
80 ℃ 10 hrs, RT 24 hrs	24	39	1572.44 ± 872.05^{C}	24.55 ± 6.20AB	3594.55

Length/ Width values in same column followed by same superscript are not statistically different per ANOVA with LSD post-Hoc testing.

3.4 SDS-PAGE

SDS-PAGE gels were utilized in order to observe the hydrolysis of proteins over time during fibril formation, allows for insight into which protein bands were broken down initially and therefore were most likely utilized in fibril formation. Depending on the condition, samples after different time intervals were loaded onto gels and hydrolysis was observed.

For the 65 ℃ stirring 4 – 20% Mini-PROTEAN® TGX™ Precast Protein gel (Figure 12, [left]), as the time the sample is sitting or stirring at 65 ℃ increases, bands in the higher kDa

range disappear and bands in the lower kDa range appear. Faint bands around 60 kDa, which correspond with conarachin, can be seen at times 1 hr, 2.5 hr, and 5 hr but disappear if held for longer than 5 hrs. Bands around 48 kDa and 40 kDa, which correspond to acidic arachin, can be seen at times 1 hr, 2.5 hr, 5 hr, 10 hr, and 24 hr but disappear completely after 24 hrs. Similarly, bands around 30 kDa and 20 kDa, which correspond to basic arachin, gradually fade with increasing incubation time but can slightly be seen at time 168 hr. At times 96 hr and 168 hr, bands less than 10 kDa become bigger and more blurred suggesting that there is a higher concentration of lower molecular weight proteins after the break down of higher molecular weight proteins over time. For the 65 ℃ stirring Mini-PROTEAN® Tris/Tricine Precast gel (Figure 12, [right]), as the time the sample is sitting or stirring at 65 ℃ increases, bands in the higher kDa range disappear and bands in the lower kDa range appear. Distinct bands are present around 40 kDa, 30 kDa, and 20 kDa at times 1 hr, 2.5 hr, 5 hr, 10 hr, and 24 hr. The bands around 40 and 30 kDa completely disappears after 24 hrs and the band around 20 kDa is present at 96 hr and 168 hr but is very faint. At times 96 hr and 168 hr there are significantly more dark bands present below ~12 kDa which suggests that the higher molecular weight bands that were present before and up to 24 hrs are breaking down into lower molecular weight segments that reappear at lower kDa after 24 hrs.

For the 80 ℃ stirring 4 – 20% Mini-PROTEAN® TGX™ Precast Protein gel (Figure 13, [left]), as the time the sample is sitting or stirring at 80 ℃ increases, bands in the higher kDa range disappear and bands in the lower kDa range appear. Faint bands around 60 kDa, which correspond with conarachin, can be seen at times 1 hr and 2.5 hr but disappear if held for longer than 2.5 hrs. Bands around 48 kDa and 40 kDa, which correspond to acidic arachin, and around 30kDa and 20 kDa, which correspond to basic arachin, can be seen at times 1 hr, 2.5 hr, and 5hr

but disappear completely after 5 hrs. At times 10 hr, 24 hr, 72 hr and 168 hr, bands less than 10 kDa become bigger and more blurred suggesting that there is a higher concentration of lower molecular weight proteins after the break down of higher molecular weight proteins over time. For the 80 ℃ stirring Mini-PROTEAN® Tris/Tricine Precast gel (Figure 13, [right]), as the time the sample is sitting or stirring at 80 ℃ increases, bands in the higher kDa range disappear and bands in the lower kDa range appear. Distinct bands are present around 40 kDa which disappear by 2.5 hrs, 30 kDa, which disappear by 5 hrs, and 20 kDa which disappear by 10 hrs. At times 72 hr and 168 hr there are significantly more dark bands present below ~12 kDa which suggests that the higher molecular weight bands that were present before and up to 5 hrs are breaking down into lower molecular weight segments that reappear at lower kDa after 24 hrs.

Overall, bands disappeared earlier in the samples heated at 80 ℃: at 65 ℃ the protein was observed to be mostly broken down by 24 hrs whereas for samples at 80 ℃ the protein was observed to be almost entirely broken down by 5 hrs. This suggests that hydrolysis occurs more quickly at a higher heat. It also appears that conarachin breaks down over a shorter time period, than arachin suggesting that conarachin may form the bulk of fibril since mature fibrils are completely formed by at least 24 hrs.

In Figure 14, there are bright bands present at around 20 kDa for the T0, 24 hr and no spin filter, and 24 hr spin filter with pH 8 buffer samples whereas there is a faint band at the same molecular weight for the 24 hr spin filter with pH 2 buffer samples. For the sample under the condition of 24 hr spin filter with pH 2 buffer, the overall bands are much fainter than the time zero, 24 hr no spin filter, and 24 hr spin filter with pH 8 buffer samples. If the experiment was done correctly – the bands in lane 8 should correspond to the peptides that comprise the

fibrils since the spin filter should have removed any substances that were in solution but did not contribute to fibril formation.

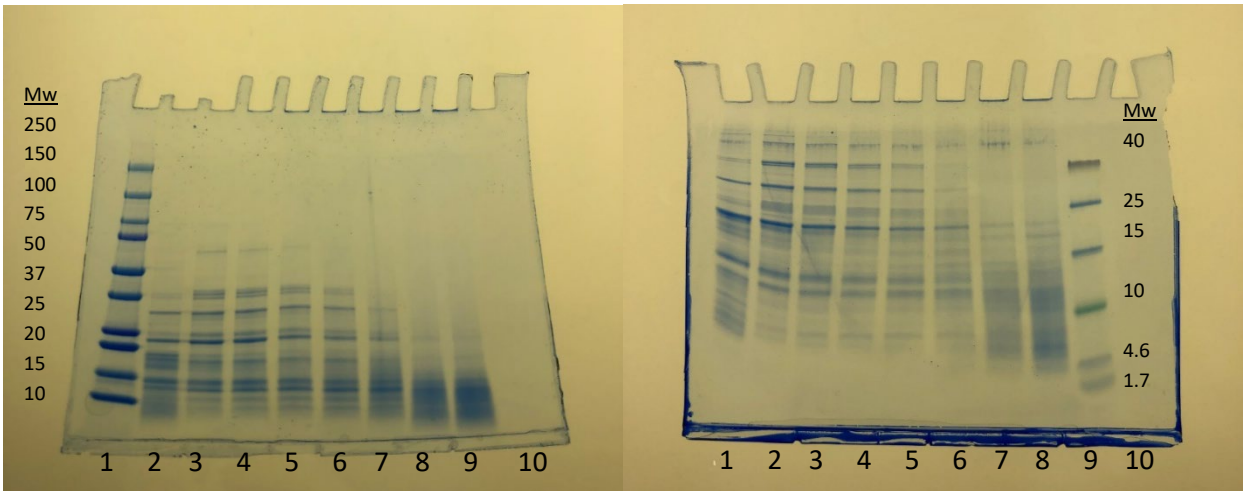

Well	1*	2	3	4	5	6	7	8	9	10
ID	L	T0	1hr	2.5hr	5hr	10hr	24hr	96hr	168	-
Volume (µL)	8	5	5	5	5	5	5	5	5	-

Figure 12. Protein Compositional Changes During Stirred Incubation at pH 2.0 and 65 °C Observed Using SDS-PAGE. HMW gel [left] and LMW gel [right] For LMW gel [right], lane 9 is ladder at 8µL and lanes 1-8 are equivalent to HWM gel [left] lanes 2-9.

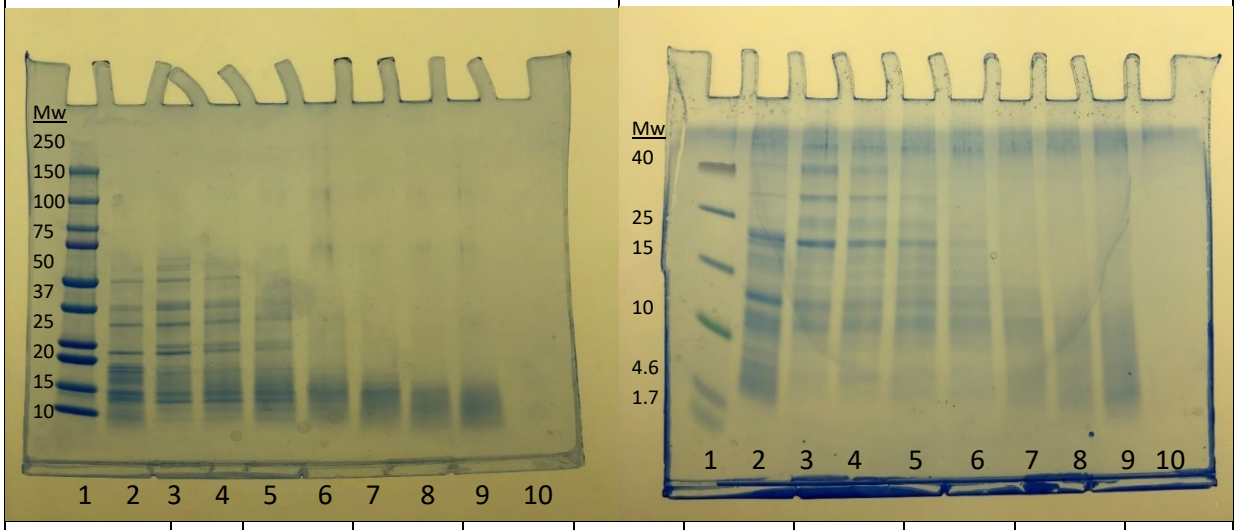

Well	1	2	3	4	5	6	7	8	9	10
ID	L	T0	1hr	2.5hr	5hr	10hr	24hr	72hr	168	-
Volume (µL)	8	5	5	5	5	5	5	5	5	-

Figure 13. Protein Compositional Changes During Stirred Incubation at pH 2.0 and 80 °C Observed Using SDS-PAGE. HMW gel [left] and LMW gel [right] For LMW gel [right], lane 9 is ladder at 8µL and lanes 1-8 are equivalent to HWM gel [left] lanes 2-9.

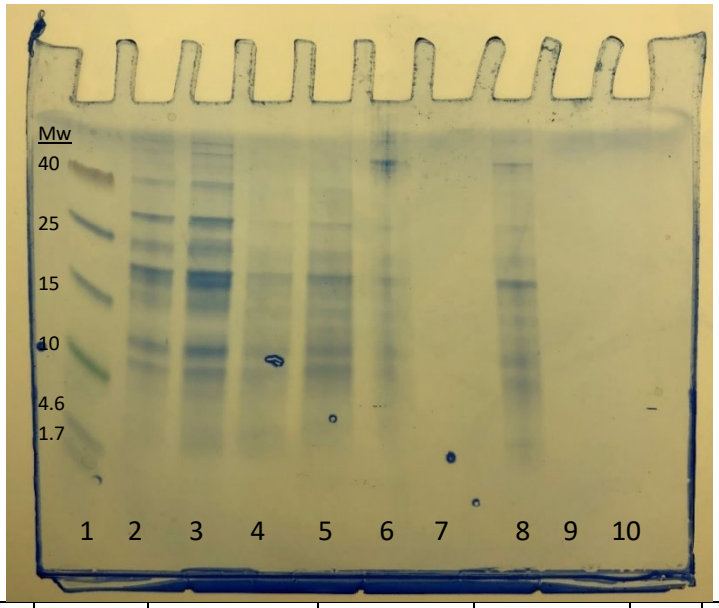

Well	1	2	3	4	5	6	7	8	9
ID	L	T0	T0	24hr no spin pH 2	24hr no spin pH 2	24hr spin pH 2	-	24hr spin pH 8	-
Volume (µL)	8	5	10	5	10	5	-	5	-

Figure 14. Protein Compositional Changes During Stirred Incubation at pH 2.0 and 80 °C, Observed Using SDS-PAGE With and Without Spin Filtration of Samples. Only low molecular weight gel was used.

3.5 Rheology

Rheology was used to observe functional characteristics of the peanut protein nanofibrils. Flow curves of viscosity vs shear rate (1/s) and shear stress vs shear rate (1/s) were determined for fibrils formed under different conditions and formed at different concentrations. Rheology data were collected in order to compare viscosity and behavior to known rheological characteristics of food protein fibrils, and are presented in Figure 15.

As seen in Figures 15A&B, samples from highest shear rate to lowest shear rate were as follows: 80 ℃ [C] stirred, 80 ℃ [C] not stirred, 80 ℃ [B] stirred, 65 ℃ [C] stirred, 65 ℃ [B] stirred, 80 ℃ [A] stirred, 65 ℃ [A] stirred, and the other samples have similar curves. For samples at the same concentration, stirring correlates with higher viscosity as compared to

samples that were not stirred. Also, samples of the same concentration and method of production (stirring vs. non-stirring) had a higher viscosity when incubated at 80 ℃ compared to 65 ℃. All flow curves show shear thinning behavior due to the shape of the curves (Akkermans et al, 2008), and all curves appear to plateau around a shear rate of 3.00 s^{-1}.

Figures 15C&Dshow the viscosity of samples from highest viscosity to lowest viscosity were as follows: 80 ℃ [C] stirred, 80 ℃ [C] not stirred, 80 ℃ [B] stirred, 65 ℃ [B] stirred, 65 ℃ [C] stirred, 80 ℃ [A] stirred, 65 ℃ [A] stirred and the other samples have similar curves. The sample under the condition of incubation at 80 ℃ with stirring and 2x starting protein concentration has the largest viscosity. Viscosity appears to increase with increased concentration of starting protein and samples held at 80 ℃ have higher viscosity than samples of the same concentration held at 65 ℃. The flow curves reached plateau at a shear rate around 10 s^{-1}.

A

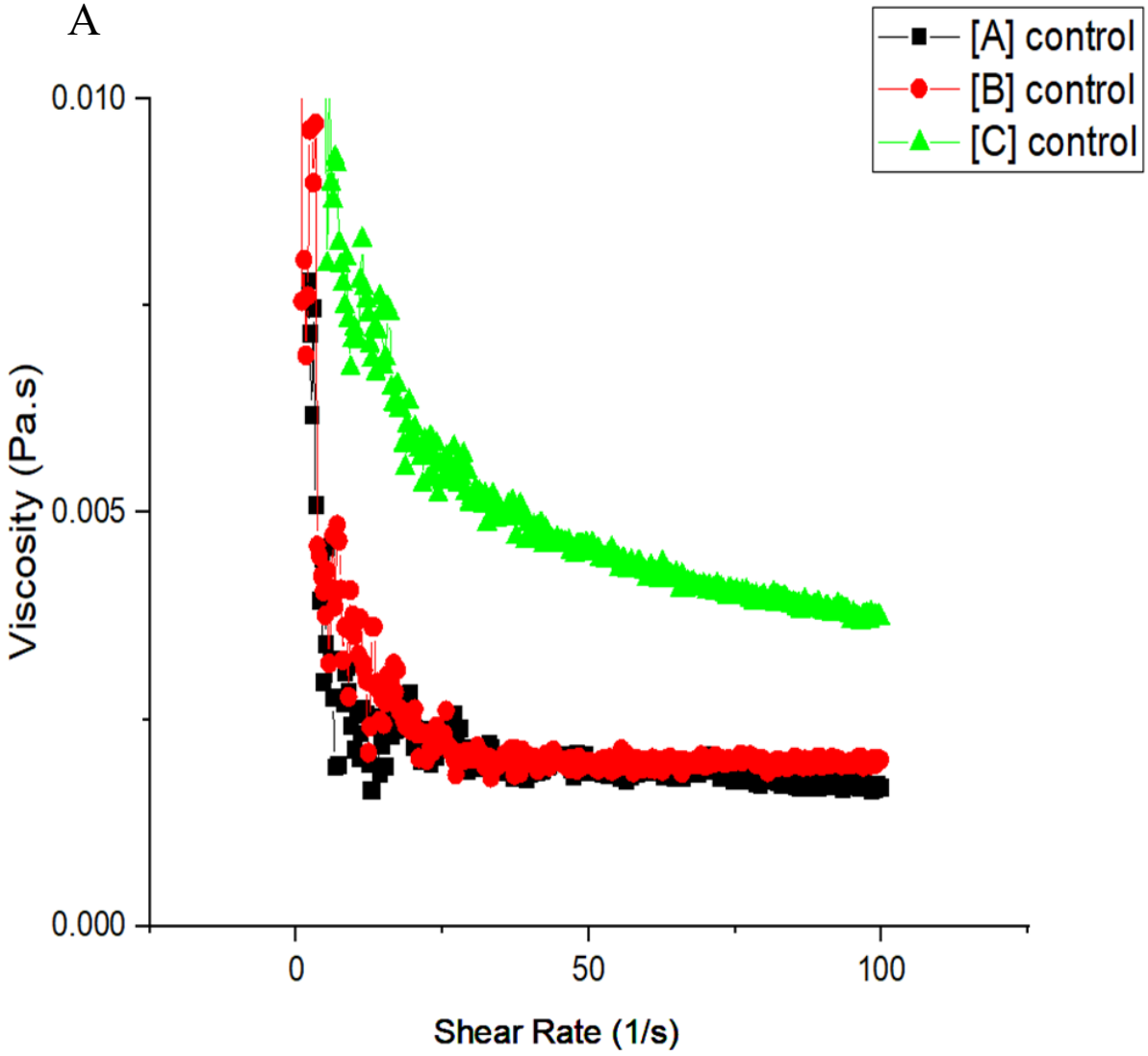
[A] control
[B] control
[C] control
0.010
0.005
0.000
Viscosity (Pa.s)
0
50
100
Shear Rate (1/s)

B

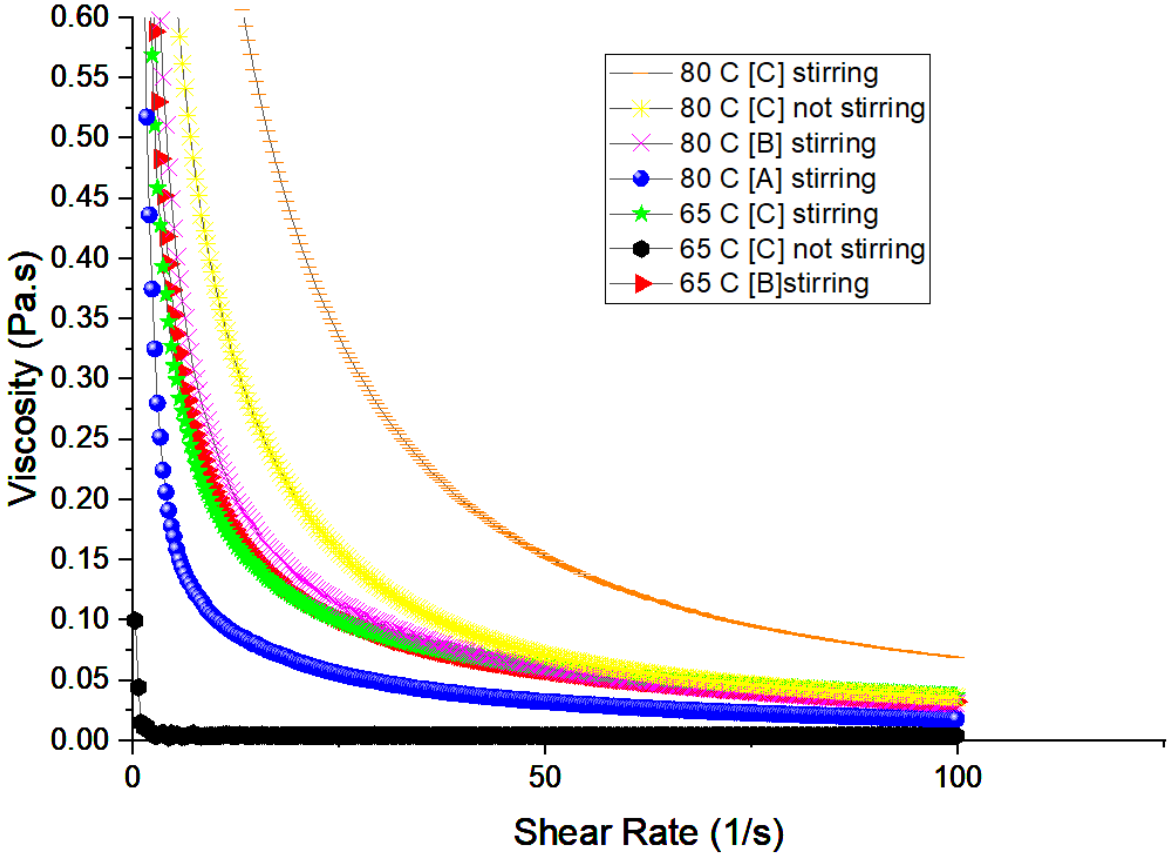
Viscosity (Pa.s)
0.60
0.55
0.50
0.45
0.40
0.35
0.30
0.25
0.20
0.15
0.10
0.05
0.00
0
50
100
Shear Rate (1/s)
80 C [C] stirring
80 C [C] not stirring
80 C [B] stirring
80 C [A] stirring
65 C [C] stirring
65 C [C] not stirring
65 C [B]stirring

C

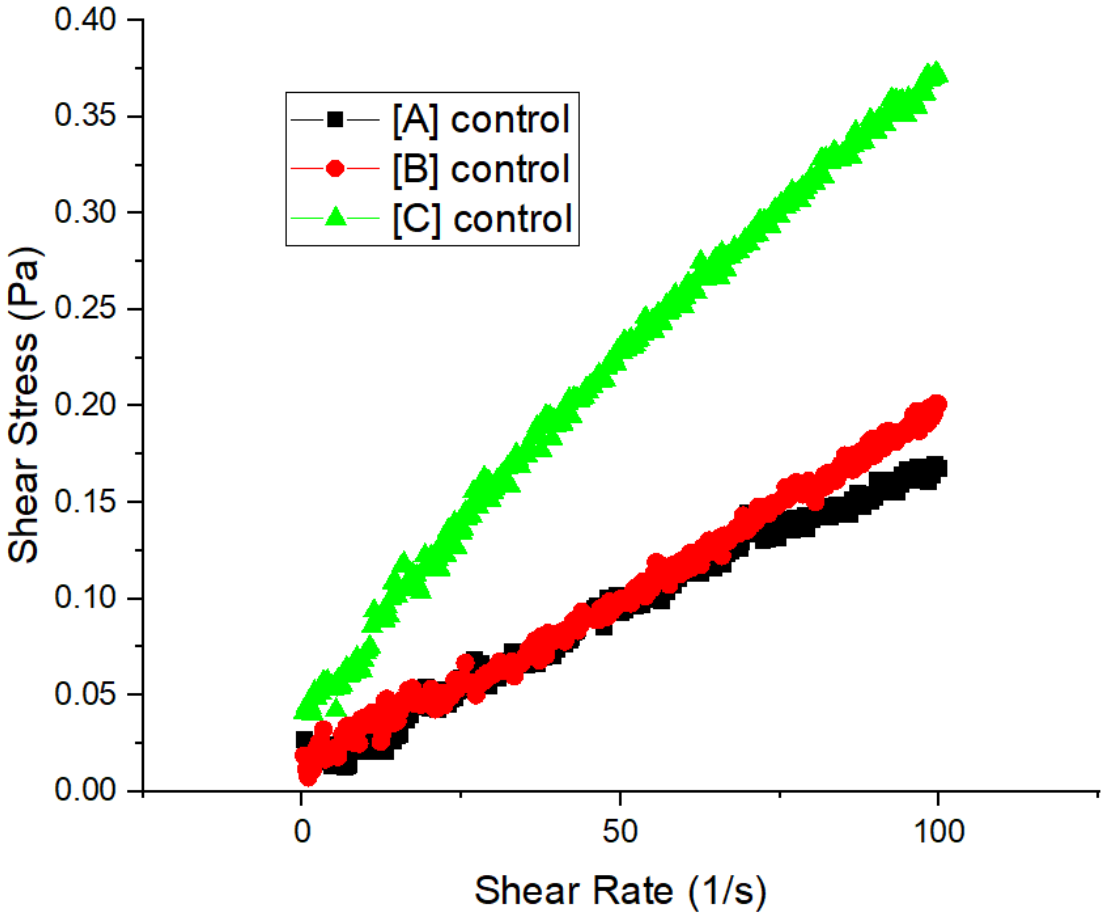
0.40
0.35
0.30
0.25
0.20
0.15
0.10
0.05
0.00
Shear Stress (Pa)
0
50
100
Shear Rate (1/s)
[A] control
[B] control
[C] control

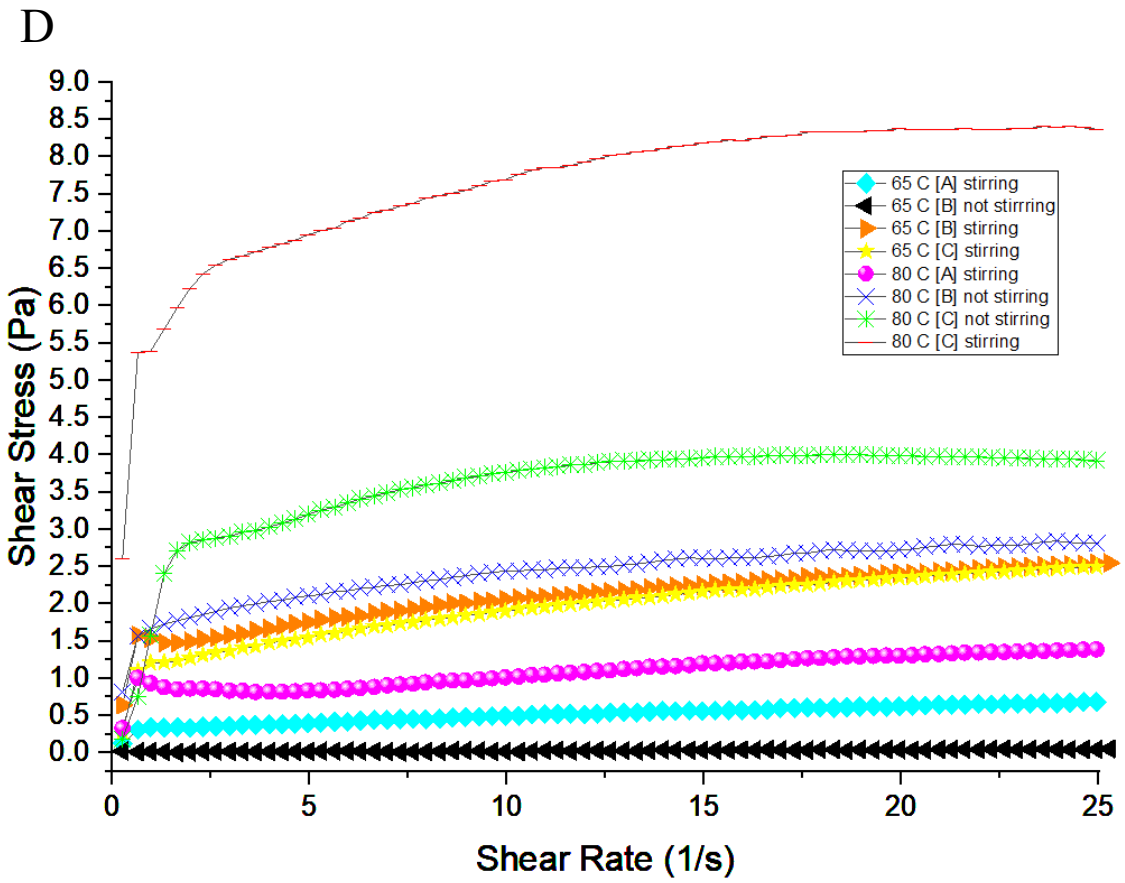

Figure 15. Rheology of Peanut Protein Nanofibrils: (A&B) shear strain (C&D) viscosity - controls are peanut protein extract that has not been incubated at difference concentrations

3.6 pH solubility

Solubility was collected in order to observe functionality of the fibrils and to compare to pH solubility of known food protein fibrils. As seen in Figure 16A, the % total ThT fluorescence for pH 2, 4, 6, and 8 are higher for the pellet compared to the supernatant. This suggests that fibrils are mostly present in the pellet or insoluble portion of the sample after changing the pH. The control, which was the non-centrifuged sample at pH 2 not separated into supernatant and pellet, had the highest ThT fluorescence and when the supernatant and pellet were sampled separately, their combined ThT fluorescence was equal to that of the control. This demonstrates that fibrils are present in both the pellet and supernatant at pH 2 but the higher intensity from the pellet suggests that most fibrils were located there although some remained soluble and were

found in the supernatant. It is important to note that for the sample of pH 2, the majority of the ThT fluorescence is found in the pellet as well suggesting that the fibril is dispersible but not fully soluble at pH 2. For samples at pH 4, 6, and 8, there is no ThT fluorescence intensity from the supernatant while in the pellet, there is similar intensity to that of the pellet from the sample at pH 2. This suggests that at pH 4, 6, and 8, the fibrils are completely insoluble.

As seen in Figure 16B, the absorbance at 280 nm is highest for the pellet for samples at pH 4, 6 and 8 and highest for the supernatant for the sample at pH 2. According to the absorbance measured, there is protein found in both the supernatant and pellet of all four samples. Since according to the ThT fluorescence data, there is no intensity from the supernatant of samples at pHs 4, 6, and 8, the protein associated with the absorbance found at 280 nm could be protein not participating in the formation of fibrils. The sum of the absorbance at 280 nm suggests that there was more overall absorbance for the samples at pH 2 and pH 4 compared to samples at pH 6 and pH 8.

As seen in Figure 16C, the highest % total protein was found in the pellet for samples at pH 4, 6, and 8 and highest for the supernatant for the sample at pH 2. This suggests that the majority of the protein in samples at pH 4, 6, and 8 is found in the pellet whereas the majority of protein in the pH 2 sample was found in the supernatant. The sample at pH 4 had the most % of total protein in the pellet, followed by pH 6, then pH 8, then pH 4, suggesting that the protein is the least soluble at pH 4, followed by pH 6, then pH 8 and most soluble at pH 2.

It is important to note that ThT intensity does not change much from pH 2 to pH 4, yet absorbance at 280 nm does change from pH 2 to pH 4. This difference in signal could be due to residual native protein still present in solution, as heating for 20 hrs at 65 ℃ does not lead to complete hydrolysis as shown in the gels above. The difference in ThT intensity and absorbance

at 280 nm could be explained by several theories. Scattering of light from precipitates could explain greater, albeit false, absorbance at 280 nm compared to ThT intensity for the same pH; hydrolysis could be breaking down the fibrils resulting in less absorbance compared to ThT intensity for the same pH, or higher absorbance at 280 nm compared to ThT intensity could be explained by the presence of protein in solution that is not participating in fibril formation.

A

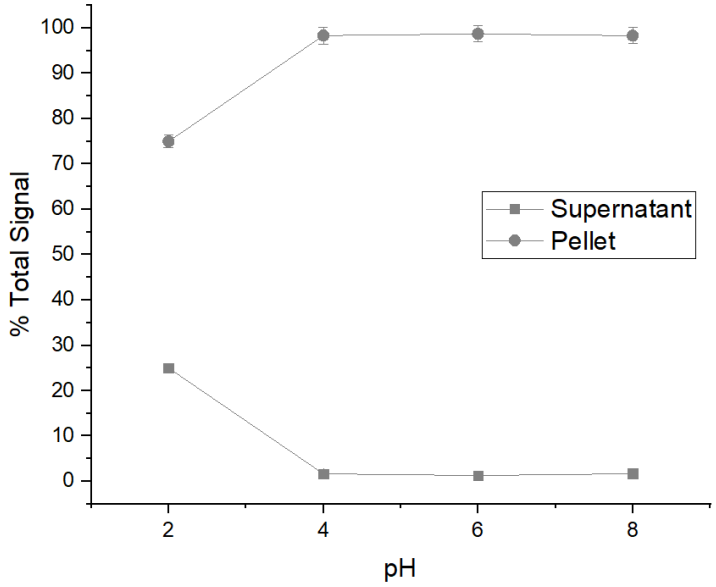

B

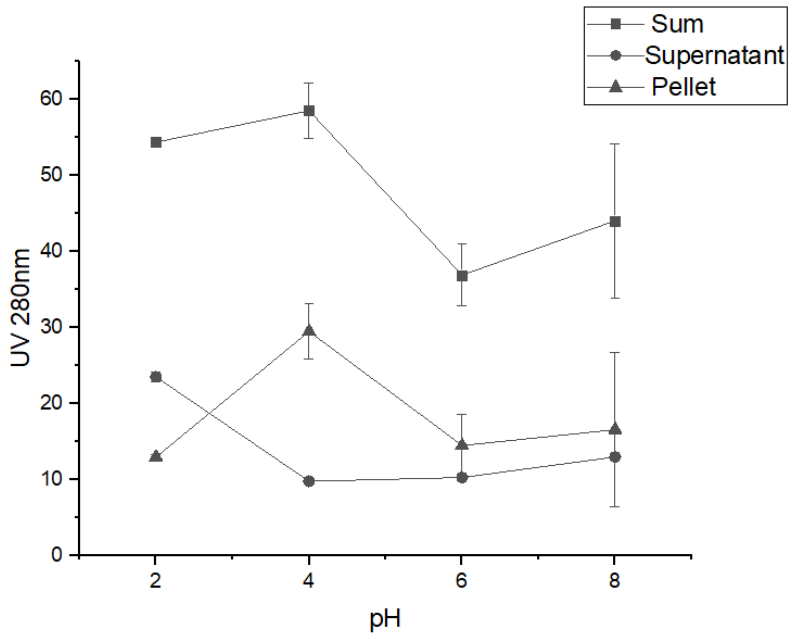

C

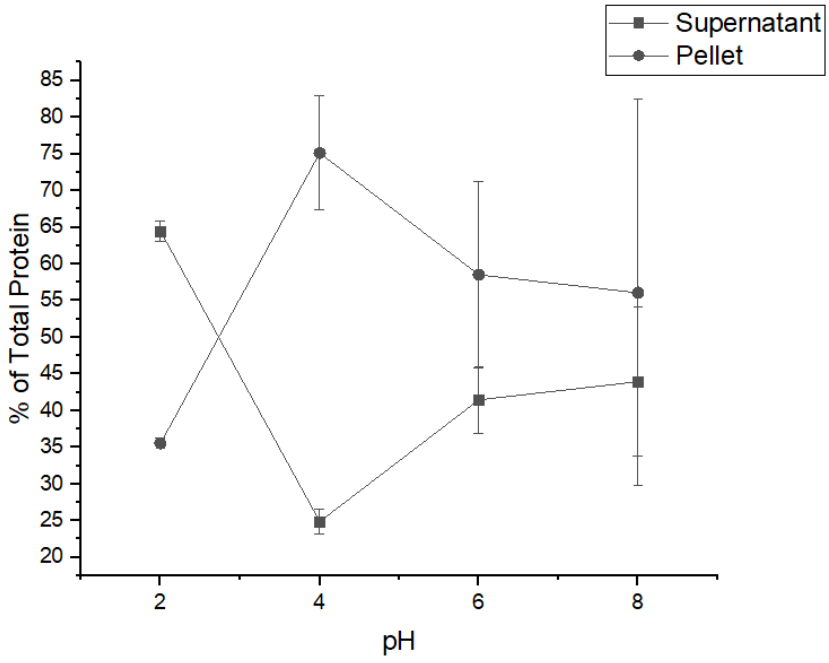

Figure 16. pH Solubility of Peanut Protein Nanofibrils. (A) ThT intensity (B) UV280 nm (C) % total protein.

CHAPTER 4

DISCUSSION

4.1 Fibril Formation Conditions and ThT Kinetics

Nanofibrils have proven to form from peanut proteins under several conditions. According to ThT fluorescence, fibrils form fastest at higher temperatures and only show a marketed increase in ThT intensity when forming while stirring, but according to TEM images, fibrils can form under both non stirring and stirring conditions. Fibrils formed without stirring were on average longer and wider – for example, fibrils incubated at 65 ℃ not stirring after 24 hrs had an average length of 3488.16 nm ± 2076.36 nm and an average width of 24.59 nm ± 5.68 nm, compared to fibrils incubated at 65 ℃ stirring after 24 hrs, which had an average length of 1280.65 nm ± 696.87 nm and an average width of 63.78 nm ± 37.44 nm. This trend of shorter and narrower fibrils over time when stirring was probably due to the shearing force of the stir bar breaking the fibrils into smaller components.

Fibrils formed at lower temperatures appeared on average longer and wider - for example, fibrils formed at 65 ℃ stirring after 24 hrs, the average length was 799.61 nm ± 523.41 nm and the average width was 30.80 nm ± 30.65 nm, for fibrils incubated at 80 ℃ stirring after 24 hrs, the average length was 957.01 nm ± 376.76 nm and the average width was 22.11 nm ± 5.69 nm. However, their length and widths were not statistically different suggesting that there is not an actual difference in length and width at different temperatures. This possible trend of shorter and wider fibrils over time at a lower temperature is most likely due to the higher temperature being a more severe environment for maturation.

Fibrils from peanut proteins appear to be able to form under similar conditions to other legume and milk proteins and have similar ThT kinetics. For example, fibrils formed from whey protein isolate (WPI) at pH 2, 80 ℃ for 22 hrs had comparable ThT fluorescence intensities and time to fibrils from peanut protein under the same conditions (Lasse et al, 2016). Fibrils formed from soy protein isolate at pH 2, 80 ℃ for 22 hr without stirring were mature after 22 hrs and had comparable ThT fluorescence intensities and times with peanut protein fibrils formed under the same conditions (Lasse et al, 2016). Also, fibrils formed for kidney bean isolate at pH 2, 80 ℃ for 22 hrs mature fibrils were formed at 22hrs of incubation and had comparable ThT fluorescence intensities and times as fibrils formed from peanut under the same conditions (Lasse et al, 2016). Peanut fibril kinetics were slower compared to that of pea protein fibril kinetics. Munialo et al, (2014) discovered that fibrils formed from pea protein at pH 2, 85 ℃ for 20 hrs with continuous stirring at 300 rpm reached maximum fluorescence intensity in the first 2 hrs which was faster than the fibrils formed from peanut protein which hit maximum intensity in about 6hrs for the condition of 80 ℃ with constant stirring and in about 15 hrs for the condition of 65 ℃ with constant stirring.

In a further breakdown of soy protein into its components, Akkermans et al, (2007) formed fibrils out of soy protein isolate (SPI), containing 80% glycinin and 20% beta-conglycinin, and glycinin, containing 90-94% glycinin and the remaining beta-conglycinin. Fibrils were formed at pH 2, 85 ℃ in a shearing device for 2 hr or 20 hr with or without shear depending on the condition desired. It was discovered that SPI had higher ThT intensity than soy glycinin which had a higher concentration of beta-glycinin. This could suggest that beta-conglycinin forms the majority of the fibril or has a more innate ability to form mature fibrils that glycinin. It is possible that the peanut protein extraction done in this experiment might have

excluded a majority of the conarachin, the peanut version of beta-conglycinin, and without the aid of stirring to form a nucleation site, the arachin, the peanut version of glycinin was unable to form mature fibrils as readily.

According to this experiment, fibrils form faster at a higher temperature: the average lag phase of fibril kinetics formed at 80 ℃ was 3.2 ± 0.1 and the average lag phase of fibril kinetics formed at 65 ℃ was 5.8 ± 3.8 suggesting that nucleation, and therefore fibril formation, occurs faster at higher temperatures. This trend can also be observed in the literature. Loveday et al, (2012) observed that fibrils formed from beta-lactoglobulin at pH 2, 75 -120 ℃ without stirring demonstrated that temperature is inversely related to lag phase. Kroes-Njiboer, et al, (2009), also, observed heating at 80-85 ℃ with continuous stirring produced significantly higher ThT fluorescence intensity after 24 hrs of incubation compared to lower temperatures.

4.2 Effects of Stirring on Fibril Formation

Bolder, et al (2007) suggested that nucleation is one of the principal reasons for fibril formation and the presence of a stir bar has the ability to form that nucleation site. This may explain why, in this study, unstirred samples showed limited or no ThT fluorescence. Further, the addition of shear flow has been shown to decrease the amount of time it takes for fibrils to form - when heating fibrils for 20 hrs, shear flow had no effect but when heating for 2 hrs, shear flow enhanced formation (Bolder et al, 2007). This ability of shearing or stirring to enhance formation in a short amount of time could explain why, in this experiment, fibrils formed with stirring, produced ThT fluorescence intensity and those without stirring did not produce any intensity. Additionally, Munialo, et al, (2014) observed an increase in ThT intensity, concluding that fibrils

form from native pea and soybean protein extracts only under constant stirring, most likely due to the presence of shearing forces.

It is possible that proto-fibrils from peanut protein may have formed in the samples without stirring, but did not have enough time to nucleate and form mature fibrils due to the absence of shearing forces. Further research on the formation of peanut fibrils without stirring is needed to observe if fibrils can form at that condition, but simply need a longer incubation/maturation time or if they cannot form at all without the presence of a shear force.

Even though ThT intensity did not increase for the unstirred samples , TEM imaging proves that some fibrils were formed. This suggests that without stirring, the concentration of fibrils formed were so low that their binding to ThT was so limited as to not show measurable increased intensity. The possibly limited concentration of fibrils further support the idea that absent a shearing force, nucleation sites are limited, and this limit affects the amount of fibrils formed.

It should be noted that Lasse, et al. (2016) was able to form fibrils from kidney bean and soybean protein isolate without stirring and also observed an increase in ThT intensity. However, these fibrils were formed from the protein isolate, which may suggest that there is some interfering factor present in the native protein extract but absent in the protein isolate extracts that impedes ThT measurements.

4.3 Hydrolysis is Central to Fibril Formation

The SDS-page gels in this experiment demonstrate that during the fibril formation process, peanut proteins are hydrolyzing into smaller protein fragments over time, which are most likely forming the bulk of the fibril. For example, at both temperatures, bands in the higher

kDa range(60 kDa, 40 kDa, etc) disappear and bands in the lower kDa range(~12 kDa) appear. This observation, along with those of Lasse, et al (2016) which showed that protein hydrolysis resulting in peptides smaller than 15 kDa after 22 hrs of incubation for soy protein isolate, kidney bean isolate, and whey protein isolate, strongly suggest that mature fibrils are generally made from smaller peptides.

Furthermore, the gels in this experiment suggest, as might be expected, that the protein breaks down more rapidly at higher temperatures, which should, and appears to result in faster formation of fibrils: notably, at 65 ℃ the protein was observed to be mostly broken down by 24 hrs whereas for samples at 80 ℃ the protein was observed to be almost entirely broken down by 5 hrs.

Furthermore, the current work shows that conarachin appears to break down over a shorter time period than arachin, which suggests that conarachin may form the bulk of fibrils, as mature fibrils are completely formed by at least 24 hrs. For example, Hydrolysis of bands around 60 kDa, which correspond to the vicilin/conarachin portion of the peanut protein, for both 65 ℃ and 80 ℃ incubation could be observed in this experiment. According to Munialo et al, (2014), hydrolysis of bands larger than 66 kDa, which correspond with the vicilin portion of the pea protein, occurred over 22 hrs of incubation. The vicilin portion for both legume proteins is hydrolyzed most readily compared to the legumin portion (Munialo et al, 2014), suggesting that the vicilin forms the bulk of the fibril.

4.4 Structure of Peanut Protein Nanofibrils

According to the collected electron micrographs, fibril characteristics followed the general trend of shorter but wider fibrils on average forming during incubations at conditions

with stirring, with incubations at a higher temperature resulting in shorter and narrower fibrils on average. Compared to fibrils formed from peanut protein, kidney protein isolate (KPI), soybean protein isolate (SPI), and pea protein fibrils were shorter and less wide as they were characterized as curly, about 8 nm wide, and 250-300 nm in length (Lasse et al, 2016). This large variance could be due to the inherent differences in the protein structures themselves or could be due to the fact that the TEM images in previous publications (produced from KPI, SPI, and pea protein) were from samples which had undergone fairly prolonged storage 7-14 days) and could have undergone breakdown of the fibrils.

As far as physical appearance, the TEM images of peanut protein nanofibrils appear mostly linear and twisted. Similarly, TEM images from pea protein fibrils are described as linear and twisted with a worm-like appearance (Munialo et al, 2014) while TEM images from soy protein isolate are described as having a more curved and branched appearance (Wan and Guo, 2019; Akkermans et al, 2007). Fibrils formed from whey protein isolate have been described as being straight, reaching several micrometers in length and 10nm width (Akkermans et al, 2009) and as being long and semiflexible associated into large entangled networks more than 10 μm long (Loveday et al, 2011). TEM images of beta-lactoglobulin are described as being several μm long, a few nm wide and mostly unbranched (Loveday et al, 2012). Fibrils formed from whey protein and beta-lactoglobulin appear the most comparable, physically, to the peanut protein fibrils which is surprising since the other proteins are legumins, like peanuts, but may suggest that the TEM platting method used in this experiment could be a better representation of the mature fibrils. These structural similarities also suggest that the peanut fibrils could be used in a functionally similar way to fibrils formed from milk proteins. It must also be noted that there is a large variance in the average lengths, widths, and persistence lengths of the peanut fibrils

measured in this study, likely due to the fact that the TEM images only represent a portion of the entire fibril population. However, multiple images with multiple fibrils were average together in order to gain a more representative sample.

The persistence lengths found in this study were significantly longer than those for soy fibrils and the large values suggest that the fibrils are very rigged with little bend. Specifically, fibrils formed from peanut protein had a persistence length ranging from 1650 – 3750 μm, while fibrils formed from soy glycinin have been reported to have an average persistence length of 2.3 +/- 1.4 μm., While these figures may be accurate, it is also possible that an overestimate of the actual persistence length was generated by the software. This error could have resulted from the software incorrectly identifying and measuring fibrils due to the previously mentioned differences in fibril morphology, and the software did not allow the user to manually go in and highlight the fibrils desired to be measured.

4.5 Control of Fibril Length and Width

Depending on the desired length and width, the conditions at which the fibrils are formed can be altered. As shown in this study, stirring the protein solution for 10 hrs and then taking the solution to room temperature without stirring for the next 24 hr can form longer fibrils in a shorter time frame. Specifically, samples kept at room temperature without stirring after stirring at 65 ℃ for 10 hrs had fibrils that were on average approximately 3x the length and approximately 2x the width of those formed under 65 ℃ stirring for 24 hrs. Samples kept at room temperature without stirring after stirring at 80 ℃ for 10 hrs had fibrils that were on average approximately 1 2/3x the length but approximately equal width of those formed under 80 ℃ stirring for 24 hrs. This suggests that keeping the samples under continuous stirring decreases

the length and, possibly, width of the fibrils, most likely due to the shearing force of the stir bars. This experiment suggests that if quick forming long fibrils are desired, starting the samples off stirring with heat allows the fibrils to form quickly and then moving the samples to room temperature without stirring is correlated with more mature, longer, and wider fibrils. Knowing how to manipulate the length, width, and persistence length of these fibrils could be significant to the functionality of these fibrils in the food industry. If longer, more entangled networks of fibrils are desired for a viscous food product, heating at a lower temperature with stirring for an initial short time period could be used. If shorter, more dispersed networks of fibrils are desired for a slightly viscous food product, heating at high temperature with stirring could be used.

4.6 Functionality

Rheological studies suggest the potential functionality of these fibrils and how they could be utilized in the food industry. For example, they have shear thinning behavior and could be used as viscosity enhancers since, depending on the protein concentration, they are highly viscous. These peanut protein fibrils can be adjusted by starting concentration or formation condition in order to achieve a desirable product, such as high/low viscosity or more/less shear thinning behavior which is important for utilization in food processing. If needed, these fibrils can be manipulated very easily in order to fit the manufacturers or processors requirements. Akkermans, et al. (2007) also suggest that whey protein isolate fibril concentration has been shown to be influenced by starting protein concentration, heating, and use of shear flow.

4.6.1 Rheology

The shear thinning behavior of the fibrils and their ability to enhance viscosity suggests that these fibrils could be used in food products in order to alter the texture profile of the product to a more desirable form. This also suggests that the viscosity and/or extent of shear thinning could be adjusted depending on the condition at which the fibrils are originally prepared, such as increasing or decreasing protein concentration, or by which the fibrils are formed (e.g. stirring vs non-stirring and increasing or decreasing temperature). Fibrils formed from soy glycinin and SPI have also been shown to exhibit shear thinning behavior and enhanced viscosity compared to samples without fibrils. Further, fibril from SPI had a higher viscosity than fibrils from soy glycinin (Akkermans et al, 2007). Fibrils formed from whey protein isolate (WPI) have also been found to be shear thinning and viscosity enhancing compared to solutions without WPI fibrils and follow the general trend of increasing viscosity with increasing protein/fibril concentration which is observed in this research. Fibrils formed from beta-lactoglobulin demonstrate shear thinning behavior and follow the trend of higher viscosity with higher temperature of incubation which is observed in this research (Loveday et al, 2012).

4.6.2 pH solubility

The pH solubility trials demonstrate that the fibrils are least soluble at pH 4 – followed by pH 6, then pH 8 and most soluble but not completely soluble at pH 2. The fibril is most likely the least soluble at pH 4 and pH 6 because the isoelectric point (pI) of the native peanut protein is around 5 (UniProtKB – Q647H2; UniProtKB – Q6PSU4) and proteins are least soluble at their isoelectric points. Proteins typically precipitate out of solution at their isoelectric points since at their pI, protein to protein interactions increase due to less water interaction and less electrostatic

forces of the molecules causing more favorable conditions for the protein to aggregate and possibly precipitate (Pelegrine, D.H.G., and Gasparetto, C.A., 2005). The dissociate does not appear to destroy the fibrils, since ThT fluorescence intensity is still observed at each pH. Compared to SPI fibrils, peanut protein fibrils may be more tolerable of a higher pH, because the ThT fluorescence intensity of peanut protein fibrils only slightly decreases at pH 4 and slightly increases at pH 6 and 8. Whereas, for SPI fibrils, fluorescence intensity slightly decreased when pH increased from 2-6 suggesting that the beta-sheet structure is stable within that pH range (Wan and Guo, 2019) and as the pH continues to rise above 6, fluorescence intensity decreases suggesting that the beta-sheets are no longer stable, and the fibrils are dissociating. Peanut protein fibrils may also be more stable at higher pHs than WPI fibrils since ThT fluorescence intensity for WIP fibrils also decrease as pH increased from 2-8 (Akkermans et al, 2008).

4.7 Future work

Future research needs to be conducted on these peanut protein fibrils in order to utilize their rheological properties in the food industry. Firstly, the digestibility of the fibrils would be significant in determining if the fibrils are properly broken down in the digestive tract to eliminate any chance of inducing other proteins into fibrilization or contributing to diseases caused by fibrils. Several food protein fibrils have already been studied for protease resistance and have varying results. After 3 hrs of pepsin proteolysis, ~75% of final residual ThT fluorescence was observed for WPI fibrils and ~50-60% fluorescence for KPI and SPI (Lasse et al, 2016).). After 3 hrs of pancreatin proteolysis, WPI fibrils were almost entirely broken down demonstrated by very little ThT fluorescence and ~40-70% fluorescence for KPI and SPI. After 3 hrs of proteinase K proteolysis, little ThT fluorescence was observed for WPI, KPI, or SPI suggesting that the fibrils were well proteolyzed. Since peanut protein shares many physical

commonalities with kidney bean and soybean and the peanut protein fibrils share may physical and rheological commonalities with WPI fibrils, the peanut protein fibrils would most likely be broken down similarly to WPI, KPI, and SPI through the digestive tract. Based on my research and comparison to others' findings, these fibrils should be able to find use in the food industry without causing foreseeable harm. Furthermore, TEM imaging of these fibrils at varying pHs such as 2, 4, 6, and 8 would allow the highlighting of the physical effects of changing pH on the fibrils in order to determine if length, width, and/or persistence length can be altered. From this study, TEM images of fibrils without stirring illustrate the formation of fibrils but little to no ThT fluorescence suggests that the fibrils are not concentrated enough to produce fluorescence. More research should be done on this observation in order to determine how to produce a high enough fibril concentration to yield ThT fluorescence. Currently, there is little definitive research illustrating the use of soybean, kidney bean, and pea fibrils in emulsions, foams, and/or as viscosity enhancers. Future studies on specific food applications of these legume fibrils should be conducted in order to get a more realistic idea of their role in food functionality. Specifically, fibrils could be used in sausage as a thickening agent in order to compare thickening ability to conventional thickeners such as xanthan gum or carrageenan. As mentioned in this study, further research on the persistence lengths of these fibrils should be conducted in order to gain more realistic values.

CHAPTER 5

SUMMARY & CONCLUSION

Peanut proteins were found to form nanofibrils under acidic pH and elevated temperatures, specifically 65 ℃ and 80 ℃, similar to the conditions of fibril formation from milk and other legume proteins. The formation of fibrils was determined by ThT fluorescence intensity for stirring samples and TEM imaging for both stirring and not stirring samples. TEM images depicted fibrils with lengths on the order of 1 μm and widths of ~20 nm which varied based on temperature and stirring or no stirring. Hydrolysis was determined to be significant in the formation of these fibrils as major proteins were observed by broken down over time through SDS-page gels. These peanut protein fibrils could be utilized in the food industry as they have shear thinning behavior, an ability to enhance viscosity, and are soluble at low pHs commonly used in food products. Further studies are necessary to ensure the safety, digestibility, and functionality of these peanut protein fibrils in the food industry but their introduction to the industry could provide an alternative to conventional viscosity enhancers and could spawn a new alternative to animal products in a market trending away from such products.

REFERENCES

1. Arosio, P., Knowles, TP., Linse, S. (2015). On the lag phase in amyloid fibril formation. *PubMed*, 17(12), 7606-7618. doi:10.1039/c4cp05563b.
2. Akkermans C., Van der Goot A.J., Venema P., Gruppen H., Vereijken J.M., Van der Linden E., Boom R.M. (2007). Micrometer-Sized Fibrillar Protein Aggregates from Soy Glycinin and Soy Protein Isolate. *J Agric Food Chem*. 55(24), 9877-9882.
3. Araghi, L. (2018). Assessing the Safety of Food Protein Nanofibrils: Cross-Seeding of Hen and Human Lysozyme Amyloid Polymorphs. *University of Georgia*.
4. Barac M., Cabrilo, S., Pesic M., Stanojevic, S., Ziliz, S., Macej, O.,, Ristic, N. (2010). Profile and Functional Properties of Seed Proteins from Six Pea (*Pisum sativum)* Genotypes. *International Journal of Molecular Sciences,* 11, 4973-4990. https://dx.doi.org/10.3390%2Fijms11124973
5. Bio-Rad Laboratories. (n.d.) Quick Start™ Bradford Protein Assay: Instruction Manual. *Bio-Rad*. http://www.bio-rad.com/webroot/web/pdf/lsr/literature/4110065A.pdf
6. Bolder, S. G., Sagis, L. M. C., Venema, P., van der Linden, E. (2007). *J. Agric. Food Chem.,* 55, 5661– 5669.
7. Cao, Y., Mezzenga, R. (2019). Food protein amyloid fibrils: Origin, structure, formation, characterization, applications, and health implications. *Advances in Colloid and Interface Science,* 269, 334-356. https://doi.org/10.1016/j.cis.2019.05.002

8. Carbonaro, M., Maselli, P., Nucara, A. (2015). Structural aspects of legume proteins and nutraceutical properties. *Food Research International*, 76(1), 19-30. https://doi.org/10.1016/j.foodres.2014.11.007.
9. Chiti, F., Dobson, C.M. (2006). Protein misfolding, functional amyloid, and human disease. *Annual Review of Biochemistry*, 75(1) 333-366.
10. Croy, R. Gatehouse, J. A. Tyler, M. Boulter, D. (1980). The purification and characterization of a third storage protein (convicilin) from the seeds of pea (*Pisum sativum* L.). *Biochem. J*., 191, 509– 516.
11. Derbyshire, E., Wright, D.J., Boulter, D. (1976). Legumin and vicilin, storage proteins of legume seeds. *Phytochemistry*, 15(1), 3-24. https://doi.org/10.1016/S0031-9422(00)89046-9.
12. Dong, S., Xu, H., Li, B., Cheng, W., Zhang, L. (2016). Inhibition or improvement for acidic subunits fibril aggregation formation from β-conglycinin, glycinin and basic subunits. *Journal of Cereal Science*, 70, 263-269. https://doi.org/10.1016/j.jcs.2016.07.002
13. Doyle, J., Schuler, M., Godette, W., Zenger, V., Beachy, R. (1985). The Glycosylated Seed Storage Proteins of *Glycine max* and *Phaseolus vulgaris*. *Journal of Biological Chemistry*, 261(20), 9228-9238.
14. Gasteiger E., Hoogland C., Gattiker A., Duvaud S., Wilkins M.R., Appel R.D., Bairoch A. (2005). Protein Identification and Analysis Tools on the ExPASy Server*; (In) John M. Walker (ed): The Proteomics Protocols Handbook, Humana Press,* pp. 571-60.

15. Gatel, F. (1994). Protein quality of legume seeds for non-ruminant animals: a literature review. *Animal Feed Science and Technology*, 45(3–4), 317-348. https://doi.org/10.1016/0377-8401(94)90036-1

16. Graham J.S., McCullough B.R., Kang H., Elam W.A., Cao W., and De La Cruz EM. (2014). Multi-Platform Compatible Software for Analysis of Polymer Bending Mechanics. *PLoS ONE* 9(4). doi:10.1371/journal.pone.0094766

17. James, A., Yang, A. (2016). Interactions of protein content and globulin subunit composition of soybean proteins in relation to tofu gel properties. *Food Chemistry*, 194, 284-289. https://doi.org/10.1016/j.foodchem.2015.08.021

18. Josefsson, L., Cronhamn, M., Ekman, M., Widehammar, H., Emmer, A., and Lendel, C. (2019). Structural basis for the formation of soy protein nanofibrils. *Royal Society of Chemistry*, 9, 6310-6319. doi: 10.1039/C8RA10610J

19. Koppelman, S. J., Vlooswijk, R. A. A., Knippels, L. M. J., Hessing, M., Knol, E. F., Van Reijsen, F. C. and Bruijnzeel-Koomen, C. A. F. M. (2001). Quantification of major peanut allergens Ara h 1 and Ara h 2 in the peanut varieties Runner, Spanish, Virginia, and Valencia, bred in different parts of the world. *Allergy*, 56, 132–137. doi:10.1034/j.1398-9995.2001.056002132.x

20. Kroes-Nijboer, A. Sawalha, H. Venema, P. Bot, A. Floter, E. den Adel, R. Bouwman, W. G. van der Linden, E. (2012). Stability of aqueous food grade fibrillar systems against pH change. *Faraday Discuss*, 158, 125– 138.

21. Lassé, M., Ulluwishewa,D., Healy, J., Thompson, D., Miller, A., Roy, N., Chitcholtan, K., Gerrard, J.A. (2016). Evaluation of protease resistance and toxicity

of amyloid-like food fibrils from whey, soy, kidney bean, and egg white. *Food Chemistry*, 192, 491-498. https://doi.org/10.1016/j.foodchem.2015.07.044.

22. Loveday, S.M., Anema, S.G. Singh, H. (2017). β-Lactoglobulin nanofibrils: The long and the short of it. *International Dairy Journal*, 67, 35-45. https://doi.org/10.1016/j.idairyj.2016.09.011.
23. Loveday, S.M., Rao, M.A., Creamer, L.K. Singh, H. (2009). Factors affecting rheological characteristics of fibril gels: the case of β-lactoglobulin and α-lactalbumin. *Journal of Food Science*, 74(3), 47-55.
24. Manning, G.S. (2006). The persistence length of DNA is reached from the persistence length of its null isomer through an internal electrostatic stretching force. *Biophysical Journal,* 91(10), 3607-3616. doi:10.1529/biophysj.106.089029
25. Malmos, K.G., Blancas-Mejia, L.M., Weber, B., Buchner, J., Ramirez-Alvarado, M., Naiki, H., Otzen, D. (2017). ThT 101: a primer on the use of thioflavin T to investigate amyloid formation. *The Journal of Protein Folding Disorders: Amyloid*, 24(1), 1-16. doi:10.1080/13506129.2017.1304905
26. Munialo, C., Martin, A., Linden, E., de Jongh, H. (2014). Fibril Formation from Pea Protein and Subsequent Gel Formation. *Journal of Agricultural and Food Chemistry*, 62, 2418-2427.
27. Nelson, R., Sawaya, M.R., Balbirnie, M., Madsen, A.O., Riekel, C., Grothe, R., Eisenberg, D. (2005). Structure of the cross-β spine of amyloid-like fibrils. *Nature: International Journal of Science*, 435, 773-778.
28. Pelegrine, D.H.G., and Gasparetto, C.A. (2005). Whey proteins solubility as function of temperature and pH. *LWT – Food Science and Technology*, 38(1), 77-80.

29. Perez, C., Miti, T., Hasecke, F., Meisl, G., Hoyer, W., Muschol, M., Ullah, G. (2019). Mechanism of Fibril and Soluble Oligomer Formation in Amyloid Beta and Hen Egg White Lysozyme Proteins. *The Journal of Physical Chemistry*, https://doi.org/10.1021/acs.jpcb.9b02338

30. Pimentel, D.; Pimentel, M. (2003). Sustainability of meat-based and plant-based diets and the environment. *Am. J. Clin. Nutr*., 78, 660S– 663S.

31. Purwanti, N., Warji, Mardjan, S.S., Yulani, S., and Schroen, Y. (2018). Preparation of Multi-layered Microcapsules from Nanofibrils of Soy Protein Isolate using Layer-by-Layer Adsorption Method. *Earth and Environmental Science*, 147. doi :10.1088/1755-1315/147/1/012009

32. Rambaran, R. N., & Serpell, L. C. (2008). Amyloid fibrils: Abnormal protein assembly. *Prion*, 2(3), 112–117.

33. Shevkani, K., Singh, N., Kaur, A., Rana, J.C. (2015). Structural and functional characterization of kidney bean and field pea protein isolates: A comparative study. *Food Hydrocolloids*, 43, 679-689, https://doi.org/10.1016/j.foodhyd.2014.07.024

34. Smith, S.C., Johnson, S., Andrews, J., McPherson, A. (1982). Biochemical Characterization of Canavalin, the Major Storage Protein of Jack Bean. *Plant Physiology*, 70, 1199-1209. https://www.ncbi.nlm.nih.gov/pmc/articles/PMC1065850/pdf/plntphys00553-0281.pdf

35. Tang, C.-H. Zhang, Y.-H. Wen, Q.-B. Huang, Q. (2010). Formation of amyloid fibrils from kidney bean 7S globulin (phaseolin) at pH 2.0. *J. Agric. Food Chem*, 58, 8061– 8068.

36. UniProt. (2018). *UniProtKB – P02856 (VCL_1PEA)*. Retrieved from http://www.uniprot.org/uniprot/P02856

37. UniProt. (2017). *UniProtKB – P02857 (LEGA_PEA).* Retrieved from http://www.uniprot.org/uniprot/P02857

38. UnitProt. (2017). *UniProtKB – F8QXP7 (F8QXP7_PHAVU)*. Retrieved from http://www.uniprot.org/uniprot/F8QXP7

39. UniProt. (2018). *UniProtKB – P02853 (PHSB_PHAVU).* Retrieved from http://www.uniprot.org/uniprot/P02853

40. UniProt. (2017). *UniProtKB – Q647H2 (AHY3_ARAHY).* Retrieved from http://www.uniprot.org/uniprot/E9LFE8

41. UniProt, (2018), *UniProtKB – Q6PSU4 (Q6PSU4_ARAHY).* Retrieved from http://www.uniprot.org/uniprot/E9LFE7

42. UniProt. (2017). *UniProtKB – P04347 (GLYG5_SOYBN).* Retrieved from http://www.uniprot.org/uniprot/P04347

43. UniProt. (2017). *UniProtKB – P25971 (GLCB_SOYBN).* Retrieved from http://www.uniprot.org/uniprot/P25974

44. UniProt. (2018). *UniProtKB – P11827 (GLCAP_SOYBN).* Retrieved from http://www.uniprot.org/uniprot/P11827\

45. Wan, Y. & Guo, S. (2019). The Formation and Disaggregation of Soy Protein Isolate Fibril: Effects of pH. *Food Biophysics*, 14(164). https://doi.org/10.1007/s11483-019-09567-1

46. Wan, Z., Yang, X., Sagis, L.M.C. (2016). Contribution of Long Fibrils and Peptides to Surface and Foaming Behavior of Soy Protein Fibril System. *Langmuir*, 32, 8092-8101. doi:10.1021/acs.langmuir.6b01511

47. Wan, Z., Yang, X., Sagis, L.M.C. (2016). Nonlinear Surface Dilatational Rheology and Foaming Behavior of Protein and Protein Fibrillar Aggregates in the Presence of Natural Surfactant. *Langmuir*, 32(15), 3679-3690. doi: 10.1021/acs.langmuir.6b00446

48. Wang, L., Liu, H., Liu, L., Wang, Q., Li, Q., Du, L., & Zhang, J. (2014). Protein Contents in Different Peanut Varieties and Their Relationship to Gel Property. *International Journal of Food Properties*, 17(7), 1560-1576. doi: 10.1080/10942912.2012.723660

49. Warji, Mardjan, S.S., Yuliani, S., and Purwanti, N. (2017). Characterisation of nanofibrils from soy protein and the potential applications food thickener and building blocks of microcapsules. *International Journal of Food Properties*, 20(1), 1121-1131. doi: 10.1080/10942912.2017.1336720

50. Xia, W., Zhang, H., Chen, J., Hu, H., Rasulov, F., Bi, D., Huang, X., Pan, S. (2017). Formation of amyloid fibrils from soy protein hydrolysate: Effects of selective proteolysis on β-conglycinin. *Food Research International*, 100(2), 268-276. https://doi.org/10.1016/j.foodres.2017.08.059

51. Xue, C., Yuwen Lin, T., Chang, D., Guo, Z. (2017). Thioflavin T as an amyloid dye: fibril quantification, optimal concentration and effect on aggregation. *Royal Society*, 4(1). doi:10.1098/rsos.160696